

1 **Model-based analysis of erosion-induced microplastic delivery from arable land to the**
2 **stream network of a mesoscale catchment**

3 Raphael Rehm^a, Peter Fiener^a

4 ^a University of Augsburg, Institute of Geography, *Alter Postweg 118, 86159 Augsburg,*
5 *Germany*

6 *Correspondance to:* Peter Fiener (peter.fiener@geo.uni-ausburg.de)

7

8 **Abstract**

9 Soils are generally accepted as sinks for microplastic (MP), but at the same time might be a MP source
10 for inland waters. However, little is known regarding the potential MP delivery from soils to aquatic
11 systems via surface runoff and erosion. This study provides for the first time an estimate of the extent of
12 soil erosion-induced MP delivery from an arable-dominated mesoscale catchment (390 km²) to its river
13 network within a typical arable region of Southern Germany. To do this, a soil erosion model was used
14 and combined with potential particular MP load on arable land from different sources (sewage sludge,
15 compost, atmospheric deposition and tyre wear) since 1950. The modelling resulted in an annual mean
16 MP flux into the stream network of 6.33°kg° in 2020, which was dominated by tyre wear (80%). Overall,
17 0.11–0.17% of the MP applied to arable soils between 1950 and 2020 was transported into the stream
18 network. In terms of mass, this small proportion was in the same range as the MP inputs from wastewater
19 treatment plants within the test catchment. More MP (0.5–1% of input between 1950 and 2020) was
20 deposited in the grassland areas along the stream network, and this could be an additional source of MP
21 during flood events. Most (5% of the MP applied between 1950 and 2020) of the MP translocated by
22 tillage and water erosion was buried under the plough layer. Thus, the main part of the MP added to
23 arable land remained in the topsoil and is available for long-term soil erosion. This can be illustrated
24 based on a ‘stop MP input in 2020’ scenario, indicating that MP delivery to the stream network until
25 2100 would only be reduced by 14%. Overall, arable land at risk of soil erosion represents a long-term
26 MP sink, but also a long-term MP source for inland waters.

27

28 **1. Introduction**

29 The global microplastic (MP) contamination of different environmental compartments is currently the
30 focus of different research fields (Nasseri and Azizi, 2022; Tian et al., 2022; Zhang et al., 2022). Among
31 these, MP in soils have increasingly received scientific attention (Chia et al., 2021; Sajjad et al., 2022;
32 Zhou et al., 2020). Microplastic is mostly referred as plastic particles or fibres in a size range of 1 to
33 5000 μm , originating from the breakdown of larger plastic items or manufacturing at this scale for
34 various purposes (Frias and Nash, 2019; Kim et al., 2021). Many MP sources have been identified for
35 soil systems. Next to tyre wear (TW), stated as the main source (Knight et al., 2020a; Sommer et al.,
36 2018), littering (Scheurer and Bigalke, 2018) and atmospheric deposition (Brahney et al., 2020) also
37 serve as MP input pathways. Arable soils in particular often experience additional MP inputs associated
38 to agricultural soil management (Brandes, 2020). Mulch films (Ng et al., 2020), the use of compost and
39 sewage sludge as organic fertilizers (Braun et al., 2021; Liu et al., 2014; Zhang et al., 2020), irrigation
40 with contaminated (waste) water (Pérez-Reverón et al., 2022), as well as MP associated with coated
41 fertilizer and seeds (Accinelli et al., 2021; Lian et al., 2021), have proven to be the main input paths. MP
42 enters the soil system mostly via the surface and is mixed into the soil column via bioturbation (Heinze
43 et al., 2022; Li et al., 2021) and, in the case of small particles, via infiltration (Li et al., 2021). In arable
44 land, it is actively mixed into the plough layer via tillage operations (Weber et al., 2022; Zhao et al.,
45 2022; Zubris and Richards, 2005). Depending on the tillage technique, the MP is worked into the soil at
46 different depths and is more or less homogenized after multiple processing (Fiener et al., 2018; Weber
47 et al., 2022). Moreover, tillage potentially leads to mechanical fragmentation of macroplastic but also
48 reduces photochemical decomposition at the soil surface and reduces MP transport via water and wind
49 (Colin et al., 1981; Corcoran, 2022; Feuilleley et al., 2005).

50 Despite the known pathways into the soil, knowledge of the fate of MP particles once they enter the
51 soil system is limited (Guo et al., 2020; Hurley and Nizzetto, 2018; Tian et al., 2022). However, the

52 question arises as to whether the terrestrial MP sink releases relevant amounts of MP for water bodies
53 via water erosion. If so, the soils, as an MP sink, could represent an important MP source for water
54 bodies. Besides very slow, not very well determined processes of plastic fragmentation (Corcoran, 2022),
55 there is also only a small number of studies analysing vertical MP transport due to bioturbation (Heinze
56 et al., 2022; Li et al., 2021) and leaching (Chia et al., 2021; Viaroli et al., 2022) within the soil column,
57 or lateral losses to other ecosystems via erosion processes (Borthakur et al., 2022; Bullard et al., 2021;
58 Rehm et al., 2021).

59 The potential lateral transport via (water) erosion processes might be analysed using existing
60 modelling techniques. Such approaches face two major challenges: modelling approaches are required
61 which allow the cumulative loss of MP to adjacent ecosystems to be determined while taking spatial
62 differences in MP contamination and site-specific erosion into account. Moreover, the long-term change
63 in MP concentrations in the plough layer should be considered, following mixing with subsoil at
64 erosional sites or burial of MP below the plough layer at depositional sites.

65 In general, there are different water erosion modelling approaches available, ranging from physically-
66 oriented models (MCST, Fiener et al., 2008; e.g. EROSION3D, Schmidt et al., 1999), which might be
67 suitable for dealing with the specific particle size and density of MP during transport in the case of
68 individual erosion events, to conceptual approaches e.g. WaTEM/SEDEM, (Van Oost et al., 2000; Van
69 Rompaey et al., 2001), which are able to consider long-term cumulative MP soil contamination and the
70 associated long-term soil and MP erosion, transport and deposition. In general, models of the first type
71 are very parameter and input data intensive and are mostly applied in small catchments, while the second
72 type of model needs less detailed data and is often used for mesoscale catchments (Nunes et al., 2018).
73 Following the requirements outlined above, conceptual, long-term approaches that account for spatial
74 variability in MP soil contamination and erosion processes seemed to be more appropriate than process-
75 oriented models to simulate the magnitude of erosion-induced MP delivery to the stream network of

76 mesoscale catchments. As MP loss below the plough layer might be also important in reducing topsoil
77 MP contamination, such a model approach should not only simulate water erosion, but also tillage
78 erosion processes leading to a reduction of the MP concentration at erosional sites and MP burial below
79 the plough layer at depositional sites. One of the few models simulating long-term water and tillage
80 erosion in a spatial context that updates the soil properties within the soil profile is the SPEROS-C model
81 (Fiener et al., 2015; Van Oost et al., 2005b). The water and tillage erosion components of the model,
82 originating from the WaTEM/SEDEM model (Van Oost et al., 2000; Van Rompaey et al., 2001), were
83 tested in several micro- and mesoscale catchments (Krasa et al., 2005; Verstraeten and Prosser, 2008).

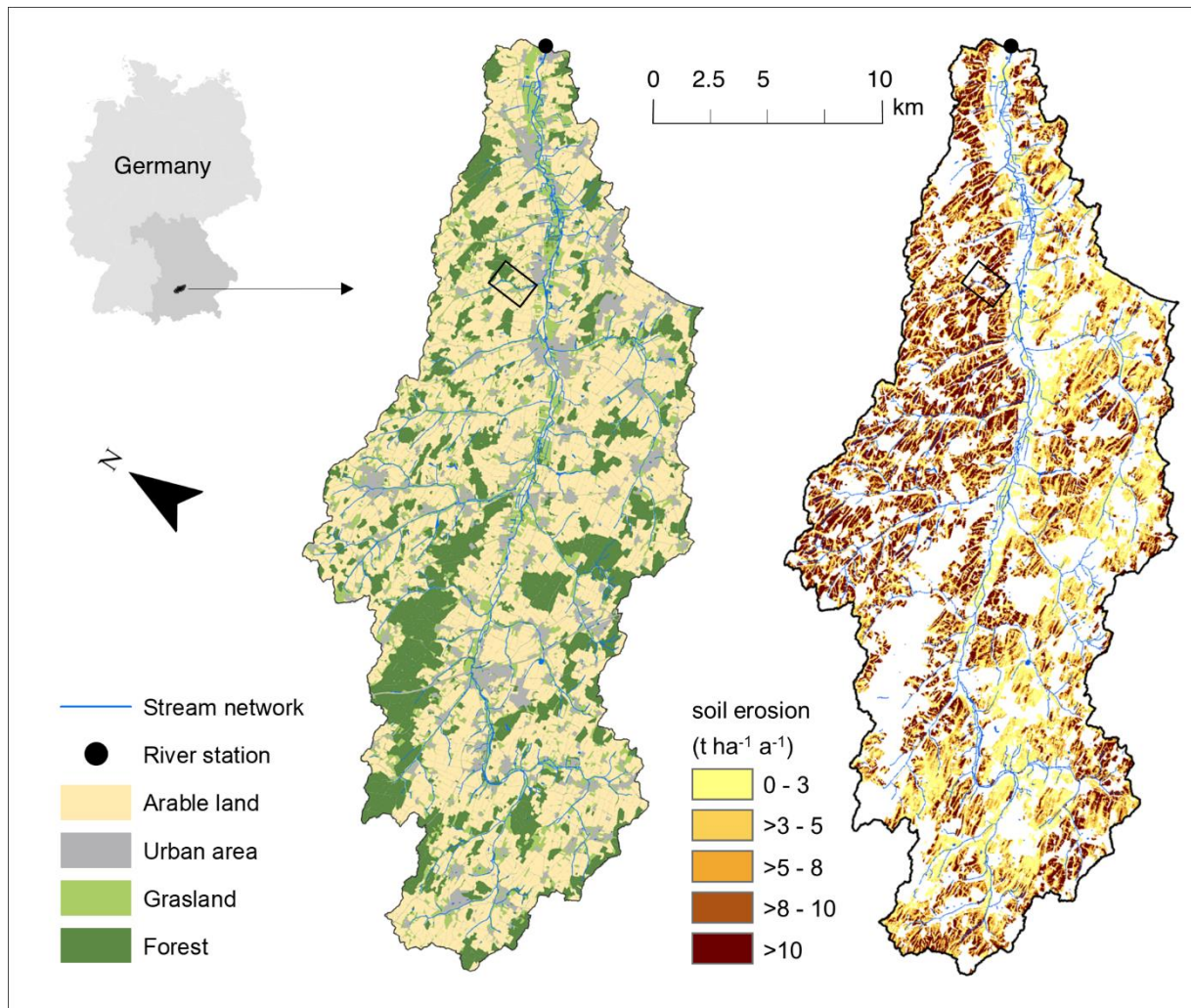
84 The general objective of this study is to investigate MP transport from arable land to the stream
85 network in an example mesoscale (390 km²) arable catchment in Southern Germany. Therefore, the
86 model SPEROS-C was adjusted to study the importance of water and tillage erosion processes for
87 particular MP transport. Specifically, this study focuses on the following areas: (i) quantifying the
88 importance of the water erosion pathway for MP input to the stream network in an example mesoscale
89 catchment, while taking into account the large uncertainties, particularly in estimates of MP input to soil;
90 (ii) determining the importance of different erosion processes in changing the MP concentration in the
91 plough layer and burying MP below the plough layer, and (iii) using scenarios to determine future
92 pathways of diffuse MP delivery into the stream network.

93 **2. Methods**

94 *2.1. Test catchment*

95 The catchment was chosen for two main reasons: (i) it represents an intensively used arable landscape
96 in Southern Germany with hilly terrain and highly productive, loess-burden soils, and (ii) the Bavarian
97 States Office for Environment has monitored discharge and sediment delivery at the outlet since 1968,
98 which allows the erosion component of the model to be tested. The mesoscale Glonn catchment

99 (48°22'N, 11°24'E) covers 390 km² and its altitude ranges from 578 m in its south-west to 447 m a.s.l.
100 at its outlet in the north-east (Fig. 1). Mean annual temperature and mean precipitation of the region are
101 7.5°C and 876 mm respectively, with the most intense rainfall events associated with convective rainfall
102 in summer. The hilly landscape ($4.7\pm 3.7^\circ$ main slope) is characterized by loamy Cambisols (WRB, 2015)
103 on the elevated terrain and loamy Gleysols (WRB, 2015) in the valleys. Land cover in this area is
104 dominated by arable land (54%), followed by forest (21%), grassland (14%) and settlements (11%) (Fig.
105 1). The main crops are arranged in a corn-grain rotation. Due to the rolling topography and the erosion-
106 prone soils, a potential long-term mean soil erosion of 5.9 t ha⁻¹ a⁻¹ (based on the German version of the
107 Universal Soil Loss Equation ABAG) could be calculated for arable land within the catchment (Lfl,
108 2023) with potential erosion rates up to 10 t ha⁻¹ a⁻¹ (Fig. 1).



109
 110 **Figure 1: The Glonn catchment (390 km²) representing a typical intensively used arable landscape**
 111 **in Southern Germany. The left and right maps show the land use and the soil erosion within the**
 112 **catchment (with a potential long-term mean soil erosion of 5.9 t ha⁻¹ a⁻¹), respectively. The black**
 113 **rectangle in the catchment marks the section of the detailed maps in Fig. 7.**
 114

115 *2.2. Model*

116 The erosion and MP transport is modelled based on a modified version of the spatially distributed
 117 water and tillage erosion and carbon (C) turnover model SPEROS-C (Fiener et al., 2015; Van Oost et
 118 al., 2005a). SPEROS-C was deliberately selected as (i) it allows the spatially explicit integration of yearly
 119 MP inputs since 1950, (ii) it routes sediment and MP through the landscape while including deposition of

120 both, and (iii) it includes water and tillage erosion as well as a yearly soil profile update (10 layers of 10
121 cm thickness) accounting for changes in MP allocation following erosion or deposition. Both, the
122 modeled deposition and the MP soil profile update allow us to analyze potential MP landscape sinks
123 either in space (e.g., in grassed areas) or in depths below the plough layer, where MP is not affected by
124 water erosion anymore.

125 The model was originally developed to analyse the long-term effect of soil erosion on landscape-scale
126 carbon balance (e.g. Nadeu et al., 2015), whereas the erosion components are based on the erosion and
127 sediment transport model WaTEM/SEDEM, which was extensively tested and validated in different
128 regions of the world (Krasa et al., 2005; Van Oost et al., 2000; Van Rompaey et al., 2001; Verstraeten
129 and Prosser, 2008). The most important model components for this study are: (i) the water erosion and
130 sediment transport component, (ii) the tillage erosion component, and (iii) the lateral redistribution and
131 the vertical mixing of MP in the soil profile following erosion and deposition processes. The model
132 component responsible for C turnover was not used and focuses exclusively on the erosion, transport,
133 and deposition of C as MP, taking into account the spatially differently distributed MP inputs from
134 different MP sources. As a result of these changes, the model is referred to as SPEROS-MP for the
135 purposes of this study. Based on the model structure it cannot account for particle size-specific selective
136 erosion, and hence, the model does not consider preferential erosion of plastic particles, depending on
137 the size, shape, density, etc. of different polymers. However, the model can account for different transport
138 pathways of different MP input sources e.g., routing tyre wear from fields along streets throughout to
139 catchment to the stream network.

140 *Water erosion component:* The water erosion component of SPEROS-MP consists of two main parts.
141 First, the erosion potential of each raster cell (5 m x 5 m) is estimated based on the German version of
142 the Universal Soil Loss Equation ABAG (Schwertmann et al., 1987). The major advantage of this well-

143 tested approach is that the input data to calculate the different USLE (ABAG) factors are available from
 144 the Bavarian State Office of Agriculture (Bayerische Landesanstalt für Landwirtschaft; LfL) and are
 145 regularly updated by the State Office administration. Sediment transport per raster cell, and hence
 146 deposition if transport capacity is smaller than sediment influx, is calculated using Eq. 1:

$$147 \quad T_c = k_{tc} \cdot R \cdot C \cdot K \cdot LS_{2D} \cdot P \quad (\text{Eq. 1})$$

148 Where T_c is the transport capacity ($\text{kg m}^{-1} \text{a}^{-1}$), k_{tc} (m) is the transport coefficient; R ($\text{N h}^{-1} \text{a}^{-1}$), C (-),
 149 K ($\text{kg h m}^{-2} \text{N}^{-1}$) and P (-) are the rainfall erosivity, soil cover, soil erodibility, and management factors
 150 of the USLE calculated for Bavaria following the approach of Fiener et al. (2020). LS_{2D} is a grid cell-
 151 specific topographic combined slope gradient and lengths factor calculated following Desmet and Govers
 152 (1996, using the digital elevation model (DEM) with a resolution of 5 m x 5 m.

153 *Tillage erosion component:* Tillage erosion is calculated based on a diffusion-type equation adopted
 154 from Govers et al. (1994), which generally assumes that tillage erosion is proportional to slope gradient
 155 (Van Oost et al., 2006):

$$156 \quad Q_{til} = -k_{til} \frac{\Delta h}{\Delta x} \quad (\text{Eq. 2})$$

157 where Q_{til} is the soil flux in $\text{kg m}^{-1} \text{yr}^{-1}$, Δh is the elevation difference in metres, Δx is the horizontal
 158 distance in meters, and k_{til} is the tillage transport coefficient in $\text{kg m}^{-1} \text{yr}^{-1}$:

$$159 \quad k_{til} = BD_i \cdot TD_i \cdot x_{til} \quad (\text{Eq. 3})$$

160 where x_{til} is the tillage translocation distance in meters, BD_i is the soil bulk density in kg m^{-3} , TD_i is
 161 the vertical depth of tillage depth in meters (0.2 m). It is important to note that tillage erosion has no
 162 direct effect on sediment or MP delivery into the stream network, but over time it modifies the MP

163 concentration in the plough layer of different raster cells, leading to a decrease in MP delivery, because
164 at erosional sites subsoil with little potential MP is mixed into the plough layer, while MP at depositional
165 sites is buried below the plough layer.

166 *MP redistribution and vertical mixing:* It is generally assumed that MP is entering the soil via its
167 surface and is immediately mixed into the plough layer (upper 0.2 m). The MP input to arable land is
168 estimated at field level (see input estimate below). For MP erosion the concentration in the plough layer
169 of each 5 m x 5 m raster cell was multiplied with the bulk soil erosion of this raster cell to calculate the
170 MP outflux to neighbouring cells. The MP concentration of the transported sediment is analogously used
171 to calculate potential MP deposition. After each year of modelling water and tillage erosion, the soil
172 profile is updated assuming a tillage operation to a constant depth of 0.2 m. Consequently, MP-free
173 subsoil is mixed into the plough layer at erosional sites, decreasing the topsoil MP concentration, while
174 at depositional sites the deposited MP is mixed with the underlying old plough layer, creating a new
175 topsoil MP concentration and some MP in the layer no longer reached by the plough. Over the years this
176 creates a steadily increasing variability in MP concentration within fields and transports MP into soils of
177 other land uses (e.g. grassland and forest sites) assumed not to get other MP inputs.

178 2.3. Data

179 2.3.1. Soil erosion model inputs and parameters

180 For the study area, the LfL provided a digital elevation model (DEM, raster 5 m x 5 m), land-use data
181 (field based), and a soil map (1:25,000) as well as most USLE factors (Tab. 1). For the sake of simplicity
182 and because long-term data on soil management was missing, only the rainfall erosivity (R factor of the
183 USLE) was calculated yearly. Therefore, we followed the approach of Schwertmann et al. (1987) using
184 a relation between annual rainfall erosivity and mean annual precipitation. Based on annual precipitation
185 available in a 1 km x 1 km grid resolution from the German Weather Service (DWD, 2020), yearly R

186 factor maps were created as model input. It is therefore important to note that the variation in model
187 sediment fluxes is solely a result of varying the annual rainfall erosivity, while changes in land
188 management (affecting the C factor of the USLE) are not considered. However, the primary focus of the
189 study was to showcase the potential magnitude and variation of MP delivery, also affected by varying
190 MP input in space and time since 1950. We assumed a corn-grain crop rotation (with a mixture of small
191 grain crops and a proportion of row crops of 25%) typically found in the region and used the USLE
192 calculator developed by Brandhuber et al. (2018), resulting in a C factor of 0.15, which is constantly
193 used for all arable land in the catchment (Tab. 1). Routing sediments from arable land to the stream
194 network, requires a sediment transport through other land uses, like forest, grassland, or paved surfaces.
195 Therefore, these land uses need to be part of the erosion modelling and hence also require a C factor. For
196 forest and grassland, a low C factor of 0.004 and for paved surfaces a C factor of 0.001 was applied
197 (Brandhuber et al., 2018). A K factor map was provided by the LfL (derived from the soil properties
198 given by the soil overview map of Bavaria at a scale of 1:25,000) based on the calculation in
199 Schwertmann et al. (1987). The LS_{2D} factor was derived from the 5 m x 5 m DEM, following the approach
200 of Desmet and Govers (1996). Assuming some soil conservation methods to be in place, e.g. partial
201 contour ploughing, the P factor was set to 0.85 (Fiener et al., 2020).

202 The values of the transport capacity coefficient k_{tc} (m) for different land use types must be generally
203 determined through calibration or taken from calibrated literature values (Dlugoß et al., 2012). Based on
204 an extensive study of Van Oost et al. (2003), who tested the sensitivity of the transport capacity
205 coefficient for different arable land and different raster resolutions, an optimum value in case of a 5 m x
206 5 m grid resolution of $k_{tc} = 150$ m was determined, which is used in this study. The author (Van Rompaey
207 et al., 2001) identified favorable k_{tc} values ranging between 0 and 60 for non-erosive landscapes at a
208 20x20 m grid, with an optimum at 42. Given my use of a finer 5x5 m grid resolution, scaled down by a
209 factor of 4, a k_{tc} value of 10 was estimated for forest and grassland.

210 The tillage transport coefficient k_{til} depends on the tillage implement, tillage speed, tillage depths, bulk
 211 density, texture and soil moisture at time of tillage (Van Oost et al., 2006). For the tillage erosion
 212 modeled, a constant k_{til} value of $350 \text{ kg m}^{-1} \text{ a}^{-1}$ for all fields was assumed (Tab. 1), which is a conservative
 213 estimate of a mixture of mouldboard and chisel ploughing (Van Oost et al., 2006).

214 **Table 1: Model parameters used in SPEROS-MP.**

| Parameters | Value | Unit | Comment | Reference |
|---------------------------------|-----------------|-------------------------------------|---|-------------------------------------|
| R | 0.048- 0.089 | $\text{N h}^{-1} \text{ a}^{-1}$ | Varies annually, controls the variability of the model | <i>DWD (2020)</i> |
| <i>C</i> | | | | |
| <i>Arable land</i> | 0.15 | - | Does not vary spatially within different land uses | <i>Brandhuber et al., 2018</i> |
| <i>Forest and grassland</i> | 0.004 | - | | |
| <i>Urban area</i> | 0.001 | - | | |
| K | 5-55 | $\text{kg h m}^{-2} \text{ N}^{-1}$ | Varies spatially depending on soil texture | <i>Fiener et al., 2020</i> |
| P | 0.85 | - | | <i>Fiener et al., 2020</i> |
| <i>ktc</i> | | | | |
| <i>Arable land</i> | 150 | <i>m</i> | Does not vary spatially within different land uses | <i>Dlugoß et al., 2012</i> |
| <i>Forest and grassland</i> | 10 | <i>m</i> | | <i>Van Rompaey et al., 2001</i> |
| <i>Urban area</i> | 0 | <i>m</i> | | |
| k_{til} | 350 | $\text{kg m}^{-1} \text{ a}^{-1}$ | | <i>Van Oost et al. 2006</i> |

215

216 2.3.2.MP contamination of soils

217 Because sampling and sample analysis would be extremely time consuming and costly, it is not
 218 possible to determine the actual MP concentrations in a 390 km^2 catchment where estimates from MP
 219 inputs suggest large spatial heterogeneity. Hence, the potential soil-MP contamination needs to be
 220 estimated from the potential MP input from different sources. As soil erosion is dominant on arable land,
 221 an MP input estimate was solely performed for arable land. However, it is important to emphasize that,
 222 except for tyre wear, estimates are based on regional means for the whole of Bavaria and that in general
 223 estimates of the MP accumulated in the catchment soils since the 1950s needs a number of assumptions

224 and simplifications, resulting in large uncertainties regarding the MP concentrations in soils. To account
225 for these uncertainties in the model outputs and arrive at a robust indication of the potential contribution
226 of soil erosion as a source of MP in the stream network, we estimated the potential yearly mean,
227 minimum and maximum soil-MP input for each input pathway (see below) and did separate (for each
228 source) and combined (for the sum of all sources) modelling runs for the different contamination
229 estimates. As mentioned earlier, mean MP inputs from sewage sludge, compost and atmospheric
230 deposition were estimated from means for all arable land in Bavaria, while input of tyre wear was derived
231 using catchment specific road data and road specific traffic data as far as possible. These represent the
232 typical sources in the agricultural landscape of Southern Germany, along with MP, applicable for
233 SPEROS-MP. Other potential MP input pathways, for instance from plastic used in agricultural
234 management (e.g. mulch films) or from littering, were not considered for two main reasons. (i) In Bavaria
235 mulch films are mostly associated with certain regions where specific crops or vegetables are grown,
236 especially asparagus. For our test site this is not the case, and using the average area of mulch cover in
237 Bavaria to estimate the potential mean input in the catchment would have resulted in very small input
238 amounts, not comparable with other regions in the world, where mulch films can be a very important
239 source of MP (Li et al., 2022; Liu et al., 2014). (ii) Larger macroplastic fragments from mulch films and
240 littering should only be transported with severe rill and ephemeral gully erosion, which are not the
241 dominant erosion processes in the region.

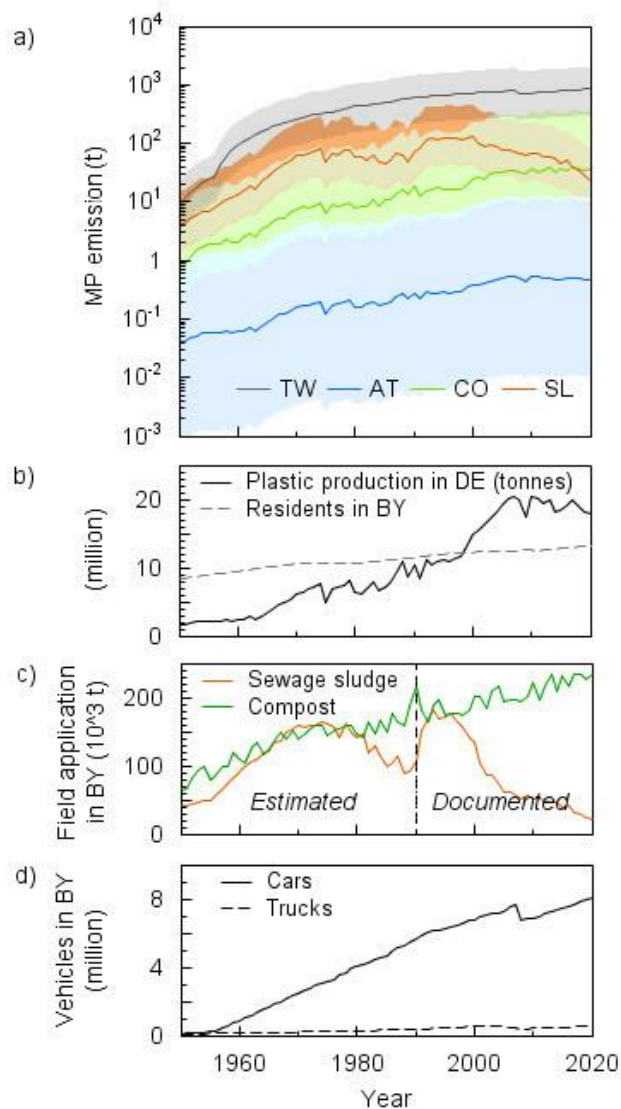
242 *2.3.3. Sewage sludge and compost*

243 Sewage sludge and compost as soil amendments (organic fertilizers) contain different quantities of
244 microplastic and, in the case of compost, small macroplastic. The first step was to estimate the amount
245 of sewage sludge and compost applied on Bavarian agricultural soils since 1950. Bavarian waste reports
246 (LfU, 1990-2020) allowed us to determine the mean annual input on arable land for the time period

247 1990–2020. Historical application rates of compost were determined based on a linear relationship
248 between application rates and population numbers between 1990 and 2020 (the variability was continued
249 at random) (LfStaD, 2022) (Fig. 2b, c). In the case of sewage sludge, the number of residents connected
250 to the sewage system was taken into account (Schleypen, 2017). The gaps between historical individual
251 values were interpolated. The development of plant technology and the use of sewage sludge between
252 1945 and 1990 were considered, as described by Schleypen (2017). While compost was constantly used
253 as an organic fertilizer, the use of sewage sludge was quite variable over time (Fig. 2c). From 1970
254 onwards new wastewater treatment plant (WWTP) technology meant that the sewage sludge was no
255 longer allowed to accumulate dry, but rather as wet sludge (Schleypen, 2017). This led to a sharp drop
256 in the use of sewage sludge as a fertilizer and it was not until the 1990s that it become popular again
257 (Fig. 2c). Since 2017, the application of sewage sludge has been largely banned in Bavaria (Schleypen,
258 2017).

259 The second step was to estimate the MP concentrations in sewage sludge and compost. To do this,
260 current literature values were used to estimate the MP concentrations for 2020. A minimum, mean and
261 maximum MP concentration was always considered, based on the range of values from literature. For
262 sewage sludge, data from Edo et al. (2020) were used; this is, to our knowledge, one of the few studies
263 providing a mass balance of MP for a WWTP by specifying the total wastewater volume and the total
264 amount of sewage sludge per day. The sum of the MP particles filtered out (contained in sewage sludge)
265 and the delivered MP from the WWTP effluent results in the number of MP detected in the WWTP input.
266 Edo et al. (2020) consider size classes 25–104 μm , 104–375 μm and 375–5,000 μm and their data show
267 that 95% of the MP in the WWTP is retained in the sewage sludge, which is consistent with other
268 publications giving ranges of 93–98% (Habib et al., 2020; Tang and Hadibarata, 2021; Unice et al.,
269 2019). For compost, data from Braun et al. (2021) were used, which contain all essential data on MP in

270 compost from Germany. They examined MP in the size ranges $< 1,000 \mu\text{m}$, $1,000\text{--}5,000 \mu\text{m}$ and $> 5,000$
 271 μm . For the mass calculation of the MP in compost, macroplastics are also included.



272 **Figure 2: a) The MP emissions for arable land in Bavaria from the different sources, tyre wear**
 273 **(TW), sewage sludge (SL), compost (CO) and atmospheric deposition (AT), from 1950 to 2020. b)**
 274 **The development of plastics production in Germany and the population of Bavaria since 1950. c)**
 275 **Amount of application of sewage sludge and compost as fertilizer on Bavarian arable land. d)**
 276 **The number of registered cars and trucks in Bavaria since 1950.**
 277

278

279 Both publications, Edo et al. (2020) and Braun et al. (2021), provide information on the size
280 distribution of the detected MP particles. This enabled the most accurate conversion possible between
281 mass and particle number. When converting, the particle size, size distribution and shape were taken into
282 account. While a spherical shape was assumed for sewage sludge, for compost the most realistic possible
283 volume for each detected particle was calculated (individual dimensions have been provided by the
284 authors of Braun et al. (2021). Based on the type of plastic detected, an average density of 1 was assumed
285 for all particles. An average MP load of 1.14 g MP kg⁻¹ dry matter of sewage sludge (min.: 0.42 g, max.:
286 4.04 g) and 0.15 g MP kg⁻¹ dry matter of compost (min.: 0.05 g, max.: 1.36 g) was assumed.

287 Based on the known amounts of sewage sludge and compost applied, it was possible to calculate the
288 corresponding amount of MP that ends up on Bavarian agricultural soils (kg m⁻²). When calculating the
289 MP concentration back to 1950, the amount of plastic produced in Germany was considered for each
290 year, as the MP concentration depends on the level of production (Fig. 2a, b). The annual amount of MP
291 was then evenly distributed across all agricultural fields in Bavaria, since spatial allocation within the
292 study area was not possible. Due to the lack of parcel-specific information before 2015 for sewage
293 sludge, we estimated MP inputs using average values per field, similar to compost. However, primary
294 aim in this modelling exercise wasn't to precisely replicate MP delivery in the Glonn catchment. Instead,
295 to demonstrate the model's use in a system analysis, acknowledging limitations in historical data
296 availability.

297 Between 1950 and 2020, a total of 7.26 million tonnes of sewage sludge and 11.7 million tonnes of
298 compost were added as organic fertilizer on agricultural fields in Bavaria. Hence it can be estimated that
299 4,090 t (min.: 1,510 t, max.: 14,500 t) and 1,110 t (min.: 358 t, max.: 10,100 t) of MP from sewage sludge
300 and compost, respectively, was dumped on arable land in Bavaria. From that, an average input on the
301 arable land in the Glonn River catchment of 42,100 kg MP from sewage sludge (min.: 15,500 kg, max.:

302 149,000 kg) and 11,500 kg MP from compost (min.: 3,660 kg, max.: 104,000 kg) was calculated. For
303 the arable land in the Glonn River catchment, this means an average annual MP application of 240 kg
304 MP from sewage sludge (min.: 90 kg, max.: 860 kg) and 370 kg from compost (min.: 120 kg, max.:
305 3,390 kg) in 2020 (Tab. 2). This results in a current entry rate of 1.14 mg MP m⁻² a⁻¹ (min.: 0.42 mg, 4.04
306 mg) from sewage sludge and 1.75 mg MP m⁻² a⁻¹ (min.: 0.56 mg, max.: 15.8 mg) from compost.

307 *2.3.4. Atmospheric deposition*

308 For the atmospheric deposition of MP, the data from four bulk deposition measurements (precipitation
309 and dust deposition) in Bavaria (Witzig et al., 2021) were combined with the development of plastics
310 production in Germany since the 1950s. Historically, the calculation of MP load relied on the assumption
311 that increased plastic production corresponds to higher emissions (Fig. 2a), although this approach is
312 notably simplified. This results in a mean cumulative atmospheric MP input on arable land in Bavaria of
313 18 tons of MP (min.: 0.41 t, max.: 407 t). Between 1950 and 2020, the arable land in the Glonn River
314 catchment was loaded with a total of 186 kg of MP (min.: 4.20 kg, max.: 4,200 kg). For 2020 an average
315 annual MP immission of 4.76 kg (min.: 0.11 kg, max.: 107 kg) or 0.02 mg MP m⁻² a⁻¹ (min.: 0.0005 mg,
316 max.: 0.5 mg) via atmospheric deposition was calculated (Tab. 2).

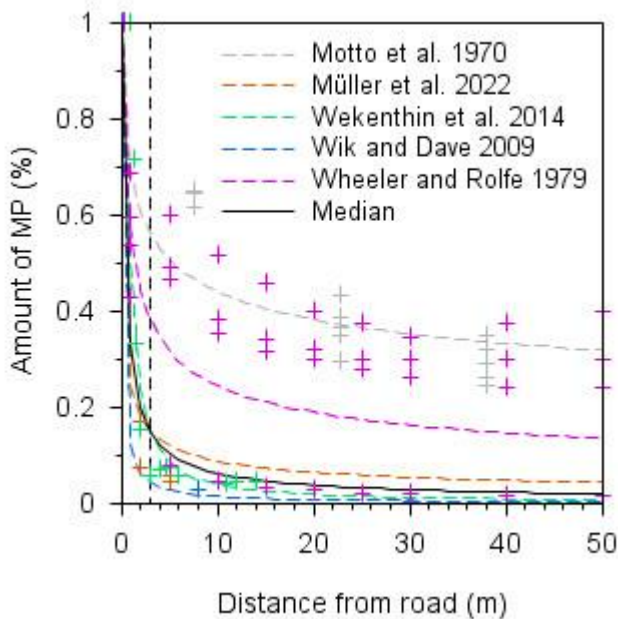
317 *2.3.5. Tyre wear*

318 To determine the tyre wear particle input in the Glonn catchment we used existing traffic counting data
319 from 2005, 2010 and 2015 for the main roads (motorways, federal roads, state roads and district roads)
320 available from the Bavarian Road Information System (BAYSIS, 2015). Traffic volume for smaller roads
321 (except farm roads) in rural areas were derived from a 1 km x 1 km population density grid following
322 Gehrke et al. (2021). Based on these data the traffic volume (number of vehicles per km) for each paved
323 road in the Glonn catchment could be estimated for the years 2005, 2010 and 2015. This was done

324 separately for passenger cars (cars), heavy-duty vehicles (trucks) and motorcycles. For all other years,
325 the traffic volume (number of vehicles per km) per road was linearly extrapolated based on the traffic
326 volume in and the number of registered cars and trucks in Bavaria (LfStaD, 2022) (Fig. 2d). No emissions
327 from unpaved roads and agricultural machinery were considered.

328 A minimum, medium and maximum scenario was considered, based on the quantity of released tyre
329 particles specified in the literature. A mean tyre wear emission factor of 90 mg TW km⁻¹ (min.: 53 mg,
330 max.: 200 mg) was assumed for cars (a motorcycle represents half a car) and 700 mg TW km⁻¹ (min.:
331 105 mg, max.: 1,7*10³ mg) for trucks, based on the reviews of Hillenbrand et al. (2005) and Wagner et
332 al. (2018). Based on the length (km) and traffic volume (number of cars, motorbikes and trucks), the
333 released TW was calculated for each section of road.

334 The transport of TW from roads into the surrounding soil systems was estimated based on literature
335 information, assuming that the TW concentration exponentially declines with increasing distance from
336 the road (Fig. 3). However, we could only identify one study (Müller et al., 2022) that directly measured
337 TW contamination of soils with distance from the road, while most other studies (Motto et al., 1970;
338 Werkenthin et al., 2014; Wheeler and Rolfe, 1979; Wik and Dave, 2009) used chemical markers and the
339 distance from the road to estimate TW distribution. From all these different approaches we calculated a
340 median behaviour (Fig. 3). As the modelling is performed in a 5 m x 5 m grid, the land-use map may not
341 show all grass or vegetation strips often found along roads, which might lead to an overestimation of
342 TW input to arable land. Hence, we decided to use a conservative estimate, assuming that at least a 3 m
343 wide grass strip can be found on both sides of any road. Consequently about 85% of the TW produced
344 on any road (Fig. 3) cannot reach arable fields. The remaining 15% of TW that could potentially reach
345 arable land mostly settles within a 50 m distance from the road, whereas background MP concentrations
346 are reached in about 130 m distance (Fig. 3).



347
 348
 349 **Figure 3: The distribution of tyre wear in the soil relative to the distance from the road. Literature**
 350 **values are based on direct detection of tyre wear (Müller *et al.* 2022) or on the estimated**
 351 **concentrations of tyre wear particles based on chemical markers (Motto *et al.* 1970, Wheeler and**
 352 **Dave 2009; Wik and Dave 2009; Wekenthin *et al.* 2014). The markers show the individual values,**
 353 **the dashed lines show the mean of the respective reference. The black line represents the median**
 354 **of all literature values used for modelling in this study.**

355
 356 In comparison to the other MP sources considered (sewage sludge, compost and atmospheric deposition),
 357 the estimate for TW was calculated on a field-by-field basis. To identify all agricultural fields affected
 358 by road-borne TW deposits within a distance of 130 m, a land-use map was overlaid on the road network.
 359 For each field, the area share of the associated road section and the distance to the road were considered
 360 when calculating the TW load. The only limitation is that on fields affected by TW, in the model the
 361 amount of TW was then distributed evenly over the entire field and not just on the affected field section
 362 near the road (within 130 m).

363 Between 1950 and 2020, $120 \cdot 10^3$ kg tyre wear (min.: $44 \cdot 10^3$ kg, max.: $289 \cdot 10^3$ kg) ended up on
 364 arable land in the Glonn catchment (Tab. 2). In 2020 the average annual MP application amounts to

365 3.1*10³ kg of tyre wear (min.: 1.1*10³ kg, max.: 7.5*10³ kg) (Tab. 2). The load from TW in 2020 can
 366 reach maximum concentrations of 2.5*10³ mg TW m⁻² a⁻¹ on roads with heavy traffic use; the average
 367 over all affected fields in the Glonn catchment area is 19.7 mg TW m⁻² a⁻¹ (Tab. 2).

368 **Table 2: MP inputs into arable soils within the test catchment, separated by different sources. All**
 369 **values are listed for the modelled time span 1950–2020 and separately for the year 2020.**
 370

| | Tyre wear | Sewage sludge | Compost | Atmospheric deposition | Unit |
|--------------------------------------|----------------|---------------|---------------|------------------------|--|
| 1950–2020 | | | | | |
| MP application to arable land | 120,256 | 42,100 | 11,500 | 186 | kg |
| min | 43,969 | 15,500 | 3,660 | 4.30 | |
| max | 288,614 | 14,9000 | 104,000 | 4200 | |
| 2020 | | | | | |
| MP application to arable land | 3,109 | 240 | 370 | 4.76 | kg |
| min | 1,137 | 90 | 120 | 0.11 | |
| max | 7,462 | 860 | 3,390 | 107 | |
| MP application rate | 19.67 | 1.14 | 1.75 | 0.02 | mg MP m⁻² a⁻¹ |
| min | 7.19 | 0.43 | 0.56 | 5*10 ⁻⁴ | |
| max | 47.2 | 4.08 | 16.03 | 0.45 | |

371

372 2.4. Model validation

373 It is obviously impossible to validate the modelled MP delivery to the stream network against measured
 374 MP loads, as this would call for a continuous monitoring of MP delivery for several years at least.
 375 However, the modelled sediment delivery can be validated against measured data from the Bavarian
 376 State Office for Environment (Bayerisches Landesamt für Umwelt, LfU), which operated a discharge
 377 and sediment monitoring gauge in Hohenkammer (Fig. 1) between 1968 and 2020. At this gauge with a
 378 defined river cross-section, daily discharge was derived from continuous runoff depth measurements in
 379 combination with a stage discharge rating curve, while the stationarity of this rating curve at the
 380 measuring cross-section was randomly checked once or twice every year. At the gauging station a weekly

381 water sample was collected (1968–2020) and its sediment concentration was determined in the
382 laboratory. From 2011 onwards a turbidity probe (Solitax ts-line; Hach Lange GmbH; Germany) was
383 installed and regularly calibrated against the samples taken by hand. Based on the continuous discharge
384 and the weekly to continuous sediment concentration measurements, the LfU provided daily sediment
385 load data for the time span 1968 to 2020, which were aggregated to yearly values for this study.

386 2.5. Modelled scenarios

387 Apart from modelling and analysing the MP delivery to the stream network via the erosion pathway
388 for the period from 1950 to 2020, we also modelled three scenarios (S1 to S3) to discuss potential future
389 pathways up to 2100.

390 *Scenario S1 – business-as-usual scenario:* In this scenario it is assumed that the MP input to arable
391 land continues until 2100 with the same input rates estimated for 2020. Given the ongoing increase in
392 plastics production (Chia et al., 2021; Lwanga et al., 2022) and rising traffic numbers (StMB, 2023), this
393 may even be a conservative estimate of a business-as-usual scenario pathway.

394 *Scenario S2 – spatially targeted application of soil amendments:* This scenario addresses two aspects.
395 (i) A potential reduction of MP delivery to the stream network due to a targeted application of soil
396 amendments, keeping a distance of at least 100 m from the stream network in the case of compost and
397 sewage sludge application. (ii) More generally illustrating the sensitivity of MP delivery to the stream
398 network in the case of non-homogenous MP inputs in the catchment. For the latter, soil amendments
399 were solely applied in the vicinity of the stream network (max distance 100 m).

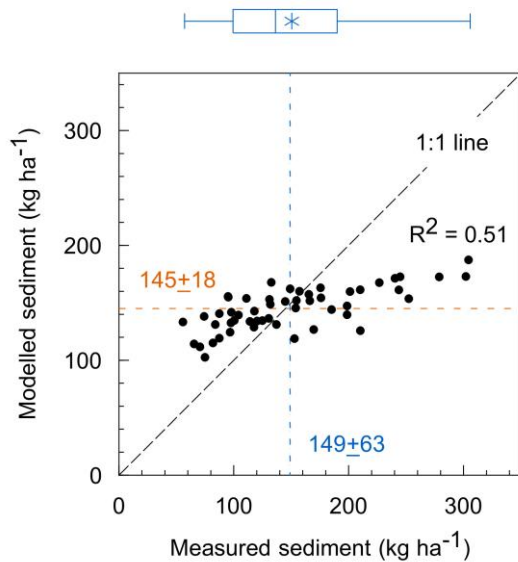
400 *Scenario S3 – stop MP input:* This scenario is set up to determine the extent to which soils function
401 as a long-term source for MP with regard to soil erosion, assuming the MP applied before 2020 remains
402 stable in the soil until 2100. Therefore, a potential decline in MP concentration in the plough layer either

403 results from a lateral loss to neighbouring land uses (grassland or forest) or the stream network, or is
404 buried below the plough layer due to deposition processes (here deposition due to water and tillage
405 erosion).

406 **3. Results**

407 *3.1. Sediment delivery*

408 Without any calibration, the model satisfactorily reproduced the measured long-term mean sediment
409 delivery of the Glonn outlet (Fig. 4). The modelled sediment deliveries resulted in a mean of 145 ± 18 kg
410 ha^{-1} , the measured mean contained 149 ± 63 kg ha^{-1} kg ha^{-1} (Fig. 4). The model was obviously not able to
411 capture the full variability in the measured yearly sediment delivery ($R^2 = 0.51$; Fig. 4). It underestimates
412 years with high erosion rates, while it overestimates years with low erosion rates. However, we conclude
413 that the model performance (especially in reproducing the long-term mean) gives a solid basis for
414 modelling lateral MP fluxes due to erosion processes. Here it is important to note that our modelling
415 approach aims to estimate the magnitude of the MP erosion transport pathway, which was not analysed
416 in earlier studies, and that the estimated MP inputs contribute significantly to model uncertainty.



417
 418 **Figure 4: Measured and modelled sediment delivery (1968 to 2020) at the outlet of the Glonn**
 419 **catchment. The blue and orange lines represent the measured and modelled means, respectively.**
 420 **The boxplots show the variability of the data. They show the median (line) and mean (star) and**
 421 **the 1st and 3rd quartile, whiskers give the minimum and maximum.**

422
 423 *3.2. MP erosion and delivery to stream network*

424 The constantly rising MP input to arable soils from different sources (Fig. 2) since 1950 is reflected
 425 in the steadily increasing, erosion-induced MP delivery into the stream network (Fig. 5a). Due to the
 426 long-term fertilization of arable land with sewage sludge, on average 0.51 kg of MP a⁻¹ entered the Glonn
 427 stream network in 2020 (Tab. 3). For compost it is 0.77 kg of MP a⁻¹, with 0.01 kg of MP a⁻¹ from
 428 atmospheric deposition (Tab. 3, Fig. 5a). With compost, sewage sludge and atmospheric deposition as
 429 potential MP inputs to arable land, SPEROS-MP generated a total MP input into the stream network of
 430 1.29 kg MP via the soil erosion pathway in 2020. Deliveries to the stream network have also steadily
 431 increased in terms of TW (Fig. 5a), with an average 5.04 kg of MP a⁻¹ delivered to the stream network
 432 in 2020 (Tab. 3).

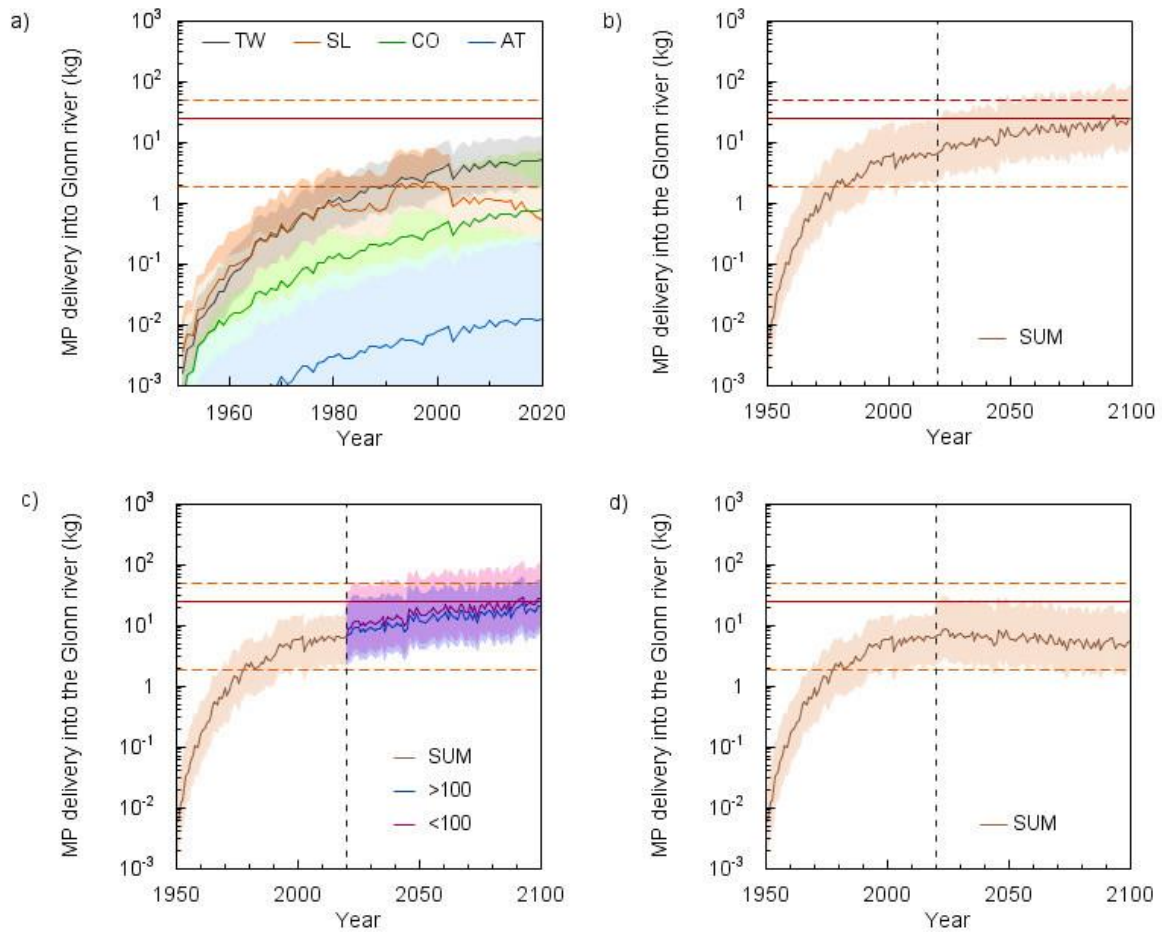
433

434 **Table 3: Soil erosion-induced MP delivery to the Glonn stream network, as well as redistribution**
 435 **to grassland and forest. The MP vertical loss below the plough layer is also given. All values are**
 436 **listed for the modelled time span 1950–2020 and separately for the year 2020.**
 437

| | Tyre wear | Sewage sludge | Compost | Atmospheric deposition | Unit |
|--|--------------|---------------|-------------|------------------------|-----------------------------|
| 1950–2020 | | | | | |
| MP delivery into stream network | 134 | 57 | 17 | 0.32 | kg |
| min | 49.0 | 21 | 5 | 0.01 | |
| max | 322 | 200 | 155 | 9 | |
| <i>Percentage of MP application</i> | <i>0.11</i> | <i>0.14</i> | <i>0.15</i> | <i>0.17</i> | <i>%</i> |
| MP delivery into grassland | 604 | 442 | 82 | 1.5 | kg |
| min | 221 | 163 | 24 | 0 | |
| max | 1,450 | 1,551 | 748 | 42 | |
| <i>Percentage of MP application</i> | <i>0.50</i> | <i>1.05</i> | <i>0.71</i> | <i>0.81</i> | <i>%</i> |
| MP delivery into forest | 108 | 97 | 18 | 0.34 | kg |
| min | 39.5 | 36 | 5 | 0 | |
| max | 259 | 340 | 164 | 10 | |
| <i>Percentage of MP application</i> | <i>0.09</i> | <i>0.23</i> | <i>0.16</i> | <i>0.18</i> | <i>%</i> |
| MP loss below plough layer | 4,703 | 2605 | 489 | 14.8 | kg |
| min | 1,720 | 961 | 144 | 6 | |
| max | 11,287 | 9,414 | 4,458 | 386 | |
| <i>Percentage of MP application</i> | <i>3.91</i> | <i>6.19</i> | <i>4.25</i> | <i>8</i> | <i>%</i> |
| 2020 | | | | | |
| MP delivery into stream network | 5.04 | 0.51 | 0.77 | 0.01 | kg MP a⁻¹ |
| min | 1.84 | 0.2 | 0.2 | 0.0003 | |
| max | 12.1 | 1.8 | 7 | 0.3 | |

438

439



440

441 **Figure 5: MP delivery into the Glonn shown individually for tyre wear (TW), sewage sludge (SL),**
 442 **compost (CO) and atmospheric deposition (AT) or the sum of TW, SL, CO and AT (SUM). The**
 443 **dashed line gives the year 2020 as the starting point for different scenarios. For comparison, the**
 444 **amount of MP delivery through wastewater treatment plants (WWTP) in 2020 is shown as a red**
 445 **line (min. and max. as dotted lines). a) MP delivery into the Glonn river between 1950 and 2020.**
 446 **b) Result of scenario S1 with the assumption that the MP input will continue as in 2020. c) Result**
 447 **of scenario S2. Compost and sewage sludge are applied to arable land at a distance of > 100 m and**
 448 **< 100 m from water streams. d) Result of scenario S3 with no MP input at all from 2020 onwards.**
 449

450 Between 1950 and 2020, 208.3 kg of MP (134 kg TW, 57 kg sewage sludge, 17 kg compost and 0.32
451 kg atmospheric deposition) entered the Glonn stream network (Tab. 3), while overall a sediment load of
452 $3.0 \cdot 10^8$ kg was delivered to the catchment outlet. TW was the main MP source, accounting for 64.3%,
453 followed by sewage sludge with 27.4%, compost with 8.2% and atmospheric deposition with 0.1%.
454 Taking into account the MP delivery relative to the MP input (i.e. total amount of MP input into soil in
455 1950–2020 vs. total MP delivery into the stream network from 1950–2020), only 0.14% of the MP
456 released to arable land was transported into the Glonn stream network. This differs slightly for the
457 different MP sources, ranging from 0.17% for atmospheric deposition to 0.11% for tyre wear (Tab. 3).

458 The spatially distributed model also allowed us to quantify the relocation of MP between different
459 land uses (an example is shown in Fig. 6f). The amount of MP delivered between 1950 and 2020 from
460 arable land to grassland and forest is $1.1 \cdot 10^3$ and $0.2 \cdot 10^3$ kg, respectively (Table 3). The larger delivery
461 to grasslands is particularly interesting, as these are mostly located along the stream network (see
462 discussion).

463 SPEROS-MP not only gives information about the MP relocation between arable land and other land
464 uses. The model also determines the amount of MP allocated buried the plough layer (and thus out of
465 reach of water erosion) at depositional sites (an example is shown in Fig. 6e). Between 1950 and 2020,
466 3.9% of the TW supplied to arable land was buried below the plough layer (Tab. 3). This corresponds to
467 $4.7 \cdot 10^3$ kg MP or 35 times the amount reaching the stream network via water erosion. For sewage sludge
468 it is 6.19% ($2.6 \cdot 10^3$ kg), for compost 4.25% (489 kg) and for atmospheric deposition 8% (14.8 kg).
469 Consequently, much more MP was buried into the subsoil than was transported into the Glonn. This
470 burial into the subsoil was caused by sedimentation via water erosion (48.5%) and tillage erosion
471 (51.5%). Conversely, up to 95% of the MP applied to arable soil over the past 70 years remains in the
472 plough layer (leaching and bioturbation excluded).



473

474 **Figure 6: Example of catchment segment (for location see Figure 1) illustrating microplastic (MP)**
 475 **input on arable land and results of erosion modelling between 1950 and 2020. The maps show the**
 476 **situation in 2020. a) Field-based land use. b) Total MP input from sewage sludge, compost and**
 477 **atmospheric input (without TW) as mean value over all arable land. c) MP input from TW,**
 478 **spatially distributed to individual arable fields. d) MP concentration below plough layer. e) MP**
 479 **transported to other land uses via soil erosion. f) MP distribution after water and tillage erosion**
 480 **on arable land. (DEM © Bayerische Vermessungsverwaltung)**
 481

482 *3.3. Scenario S1 – business-as-usual*

483 If arable soils continue to be loaded with MP the same as in 2020, the annual MP delivery rate into the
484 Glonn stream network will increase by a factor of 4 by 2100. In 2100, 25.2 kg MP a⁻¹ (min.: 9.03 kg;
485 max.: 84.1 kg) through TW, compost, sewage sludge and atmospheric deposition would end up in the
486 stream network (Fig. 5b). Between 1950 and 2100, this would make a total MP input of 1.32 *10³ kg MP
487 (min.: 511 kg; max.: 4.7 *10³ kg) into the stream network.

488 *3.4. Scenario S2 – spatially targeted application of soil amendments*

489 In S2 MP inputs from atmospheric deposition and TW accumulation continued like in S1. However, the
490 location where the organic fertilizer (sewage sludge and compost) was applied in the catchment was
491 changed. All organic fertilizers were either applied at a distance of at least 100 m from the stream network
492 or within a distance smaller than 100 m along the stream network.

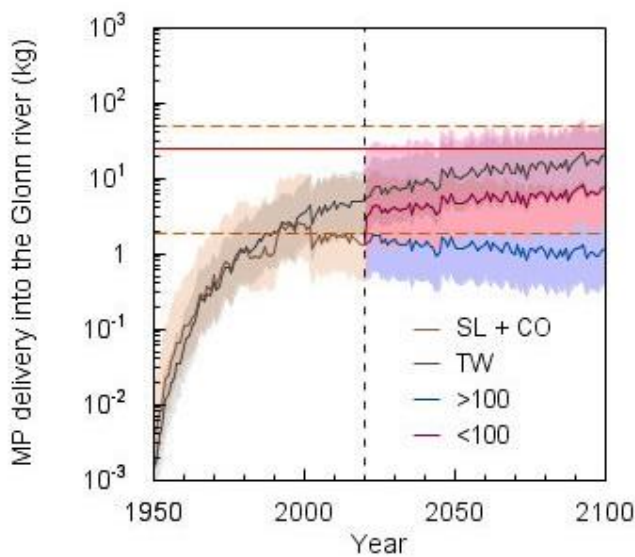
493 With an application at a distance of > 100 m, the MP delivery in the stream network would be reduced
494 to a total of 21.2 kg (min.: 7.72 kg; max.: 55.9 kg) in 2100 (Fig. 5c). That would correspond to a reduction
495 of 16% compared to S1. In the case of application at a distance of < 100 m, on the other hand, it would
496 be 27.9 kg (min.: 10 kg; max.: 102 kg) in 2100 and thus an increase of 10.7% compared to S1 (Fig. 5c).

497 The result becomes clearer if we consider TW and the organic fertilizers separately. If the distance is >
498 100 m, the annual MP delivery rate from organic fertilizer (sewage sludge and compost) without TW is
499 1.1 kg MP a⁻¹ (min.: 0.4 kg, max.: 7.8 kg) in 2100 (Fig. 7). For 2100, this would result in a 78% reduction
500 of the annual MP delivery rate from organic fertilizer into water bodies compared to S1. In total from

501 1950 to 2100, 173 kg MP (min.: 60 kg; max.: $1.0 \cdot 10^3$ kg), or 46% less MP, from organic fertilizer would
 502 end up in the stream network until 2100 (the effect of atmospheric input is negligible).

503 If organic fertilizer is applied along the stream network (max. distance < 100 m), a MP delivery of 7.8
 504 kg a^{-1} (min.: 2.6 kg, max.: 54 kg) is modelled in 2100 (Fig. 7). Between 1950 and 2100 a total of 493 kg
 505 MP (min.: 168 kg; max.: $3.25 \cdot 10^3$ kg) would be delivered to the river system by organic fertilizer
 506 (without TW).

507



508 **Figure 7: Result of scenario S2 individually shown for tyre wear (TW) and for sewage sludge**
 509 **(SL) plus compost (CO) together as organic fertilizer applied to arable land at a distance of > 100**
 510 **m and < 100 m from water streams. For comparison, the amount of MP delivery through**
 511 **wastewater treatment plants (WWTP) in 2020 as red lines (min and max as dotted lines).**
 512
 513

514 3.5. Scenario S3 – stop MP input:

515 In scenario S3 MP input stops from 2020 onwards. This abrupt stop in plastic immission is not reflected
 516 in the MP delivery rates after 2020 (Fig. 5d). However, in the year 2100, 5.43 kg of MP a^{-1} (min.: 1.98
 517 kg, max.: 18.2 kg) would still end up in the stream network from arable land due to soil erosion (Fig.

518 5d). This corresponds to a decrease in the annual MP delivery rate of 14% between 2020 and 2100, with
519 80 MP-free years (since 2020). Since 1950, a total of 684 kg MP (min.: 246 kg; max.: $2 \cdot 10^3$ kg) would
520 have ended up in the Glonn stream network.

521

522 **4. Discussion**

523 *4.1. Modelled erosion rates (sediment delivery)*

524 The modelling approach used, with a yearly time step and the missing temporal and spatial variability
525 of most model input data (especially the constant crop cover factor), while only varying yearly rainfall
526 erosivity, leads to model outputs that do not capture the full temporal dynamics of the measured yearly
527 sediment delivery. Averaging the model input variables led to an overestimation of years with low
528 sediment delivery and an underestimation of years with high sediment delivery (Fig. 4). It is well
529 documented that averaging model input variables over space and time generally leads to the
530 overestimation of years with low sediment delivery and underestimation of years with high sediment
531 delivery (Keller et al., 2021; Meinen and Robinson, 2021). The reduced temporal variability in modelled
532 sediment delivery is expected for two main reasons: (1) the annual model time step averages out years
533 where individual extreme events dominate the yearly sediment delivery, and (2) varying only the annual
534 rainfall erosivity, while all other input parameters (especially cropping dynamics) are kept constant,
535 cannot capture the temporal dynamics. However, without any model calibration the model is able to
536 reflect the long-term mean sediment delivery between 1968 and 2020 (Fig. 4), explaining 51% of the
537 variability in the measured data. Hence, we conclude that SPEROS-MP is robust enough for this
538 modelling study which focusses on MP delivery to the stream network in the Glonn catchment, especially

539 as uncertainties associated with the erosion modelling are in any case smaller than the uncertainties
540 associated with estimates of MP immissions to the arable soils in the catchment.

541 *4.2. Plausibility of MP soil input estimates*

542 Estimating the cumulative MP-soil immissions from different sources for a period starting from 1950
543 is of course associated with large uncertainties. To account for these uncertainties, we deliberately used
544 large ranges of possible inputs in our semi-virtual catchment approach which in the following discussion
545 are compared with literature values for Germany or Bavaria as a whole.

546 *4.2.1. MP from sewage sludge, compost and atmospheric deposition*

547 Brandes et al. (2021) calculated mean MP inputs into agricultural soils in Germany for compost
548 (1990–2016) and for sewage sludge (1983–2016). For Bavaria, their calculation results in compost-MP
549 input rates of between 15 and 80 mg MP m⁻² a⁻¹ and sewage sludge-MP input rates between 0 and 190
550 mg MP m⁻² a⁻¹. Bertling et al. (2021) also determined MP immissions (TW excluded) to agricultural soils
551 in Germany, resulting in much higher input rates for 2021 for compost and sewage sludge, with up to
552 702 mg MP m⁻² a⁻¹ and 2.1*10³ mg MP m⁻² a⁻¹, respectively. In contrast to the first authors, Braun et al.
553 (2021) calculate the possible MP load for the legally permissible amount of compost applied to fields in
554 Germany. This maximum permissible amount of compost application results in maximum possible entry
555 rates ranging from 34 to 4.7*10³ mg MP m⁻² a⁻¹ into agricultural soils via compost.

556 For this study, an MP emission to arable soils of between 0.42 and 4 mg MP m⁻² a⁻¹ for sewage sludge
557 and between 0.56 and 15.8 mg MP m⁻² a⁻¹ for compost were calculated for Bavaria. Our values are not
558 based on the maximum possible limits, but on the most realistic estimates possible. Therefore, our MP
559 loads remain well below the literature values. Nevertheless, the MP input from compost is likely to be

560 underestimated, based on optical detection of MP > 1 mm (Bläsing and Amelung, 2018; Braun et al.,
561 2021; Weithmann et al., 2018). Currently, much more compost ($21 \cdot 10^7$ t in 2020) is spread on fields in
562 Bavaria than sewage sludge ($24 \cdot 10^4$ t in 2020), causing higher MP emissions from compost (Fig. 2a).
563 This results from the reduction in sewage sludge application, which has been largely banned in Bavaria
564 since 2017 (Schleypen, 2017) (Fig. 2c). However, regional policy strategies regarding the use of sewage
565 sludge differ substantially within Germany, making comparisons within the country somewhat difficult
566 (Brandes et al., 2021).

567 For atmospheric deposition, an average of 771 and 395 MP particles $\text{m}^{-2} \text{d}^{-1}$ were measured at rural
568 locations in London and Hamburg (Klein and Fischer, 2019; Wright et al., 2019). Brahney et al. (2020)
569 show that airborne microplastic particles accumulate at minimum concentrations of 48 ± 7 MP particles
570 $\text{m}^{-2} \text{d}^{-1}$ even in the most isolated areas of the United States (national parks and national wilderness areas).
571 Even in Antarctic snow up to 29 MP particles per melted litre were found (Aves et al., 2022). In this
572 study, the values of Witzig et al. (2021) were used to estimate the MP contribution via atmospheric
573 deposition. They made MP measurements at different locations in Bavaria, ranging from 74 ± 19 to
574 109 ± 16 MP particles $\text{m}^{-2} \text{d}^{-1}$. Even if the transfer of such particle numbers to mass inputs is associated
575 with additional uncertainties, these amounts are orders of magnitude smaller than the inputs from sewage
576 sludge and compost. In general, taking the considerable uncertainty in the data on MP inputs via the
577 atmosphere into account, the results show that this magnitude is negligible compared to other sources
578 investigated. This finding is important in a scientific context as it provides a better understanding of the
579 magnitude of these inputs. The modelling analysis clearly shows that in comparison to other MP sources
580 the atmospheric inputs are of minimal importance.

581 *4.2.2. Tyre wear*

582 The large MP mass resulting from tyre wear is noticeable in both the TW input data and the TW
583 delivery rates into the stream network via erosion from arable land. With modelled mean TW delivery
584 of 5 kg MP a⁻¹ in 2020 into the river system, the equivalent of half a car tyre ends up as MP in the Glonn
585 (flow length of 50 km) each year. However, the calculated mean TW input to the Glonn catchment of
586 200 mg MP m⁻² in 2020 is in same the range as the estimates in other studies. For example, annual values
587 of between 180 and 370 mg TW m⁻² were reported for Germany (Baensch-Baltruschat et al., 2020;
588 Kocher et al., 2010; Wagner et al., 2018). The modelled MP input (see Fig. 3) to arable land in the Glonn
589 catchment was substantially smaller, with a mean of 19.7 mg TW m⁻².

590 Most of the TW remains on the roads or in the immediate vicinity. Some of the TW is expected to be
591 transported directly into surface waters via runoff from the road. Baensch-Baltruschat et al. (2020)
592 estimated that 12–20% of the tyre wear released on German roads ends up in surface water via road
593 runoff. The hydrological model estimates of Unice et al. (2019) indicated that 18% of released tyre wear
594 was transported to freshwater in the Seine River catchment. In comparison, when focusing on the erosion
595 of MPs mixed into the plough layer, only 0.11% of the applied TW to arable soils from 1950 to 2020
596 reached the river system. While TW represents the largest entry source in our study, the overall MP flow
597 to the stream network is an underestimation given the simplified approach. This mostly results from our
598 assumption that all roads are surrounded by a 3 m grass buffer strip (even if this was not shown in the 5
599 m x 5 m land-use raster map used), always trapping at least 85% of the TW emissions (Fig. 3). Yet even
600 this conservative assumption is associated with high uncertainties. The width of the grass strip between
601 the road and the field has an enormous impact on the MP emission. A 2 m wide buffer strip would still
602 retain approximately 80% and a 1 m wide buffer strip approximately 65% of the TW emission (Fig. 3).
603 Without any assumed grass buffer strips, the MP emission from TW would be 8 times higher. Ultimately,
604 the spatially distributed tyre wear is still associated with uncertainties. The level of TW emissions into

605 the environment (not just arable land) makes other MP sources almost negligible, especially in terms of
606 MP saving strategies.

607 Overall, it can be concluded that our estimates of MP input to the Glonn catchment are in the same
608 order of magnitude, or somewhat smaller, compared to most other studies, and hence should be more or
609 less reasonable, even if any estimates are associated with large uncertainties (e.g. extrapolating back to
610 1950; the small number of studies available for estimating MP concentrations in sewage sludge and
611 compost; errors when transferring particle numbers in particle mass etc.). However, an error in modelling
612 the MP delivery into the stream network of the test catchment most likely results from the fact that mean
613 application rates (sewage sludge, compost) for the whole of Bavaria were used (Fig. 6b), while only TW
614 input was calculated on a catchment-specific basis (Fig. 6c). Again, it is important to note that the Glonn
615 catchment was used as an example to address and discuss the potential magnitude of the MP/soil erosion
616 pathway in such mesoscale catchments determined by arable land use.

617 It should be noted that TW as not-agriculture MP-source is of paramount importance compared to
618 other MP sources, especially with respect to MP reduction measures. Not only for soil, but also for water
619 bodies and probably all other environmental compartments. Measures to prevent MP in soil will have
620 little noticeable effect if TW remains unchanged. This problem should be given more consideration in
621 future studies and interpretation of results (Knight et al., 2020a; Knight et al., 2020b; Mennekes and
622 Nowack, 2022).

623 *4.3. The modelled fate of MP*

624 As a mass-balanced model, SPEROS-MP calculates the MP input in mass (kg m^2) and not in particle
625 numbers. Hence, the model does not consider the type, shape, density, size or chemical properties of the
626 MP particles from different MP sources. It thus treats the erodibility of MP from all input pathways

627 equally. However, it can be assumed that particle properties play a decisive role for the erosion-induced
628 lateral transport, as well as for the potential vertical transport. Small MP particles should be translocated
629 faster below the plough layer due to bioturbation and maybe infiltration (Li et al., 2021; Rehm et al.,
630 2021; Waldschläger and Schüttrumpf, 2020). A subsequent reduction in MP concentration in the plough
631 layer will also reduce MP erosion. On the other hand, smaller MP particles might more strongly interact
632 with soil organic or mineral particles, or might even be included in soil aggregates, hence are more likely
633 transported as bulk soil. For example, Rehm et al. (2021) were able to demonstrate in a long-term plot
634 experiment that smaller PE particles (53–100 μm) are less strongly enriched in delivered sediments
635 compared to larger PE particles (250–300 μm). Such behaviour might change again with increasing
636 particle size, because if particles transported with sheet flow are larger than the flow depths (mostly < 1
637 mm), transport in suspension is no longer possible.

638 In general, the potential decrease in topsoil MP concentration due to infiltration and bioturbation is
639 not accounted for in SPEROS-MP. Vertical MP transport via infiltration and bioturbation has been
640 widely discussed and partially observed in earlier studies, e.g. (Rillig et al., 2017), while earthworms
641 play an especially important role in directly transporting MP via digestion and excretion (Huerta Lwanga
642 et al., 2017) or in preparing preferential flow pathways for MP leaching (Yu *et al.*, 2019). Ignoring these
643 processes of vertical movement below the plough layer will potentially lead to a slight overestimation of
644 the topsoil MP concentration in the modelling approach presented here.

645 SPEROS-MP not only delivers MP into the stream network, but also redistributes MP within the
646 catchment and within the soil profile. As arable land in the catchment is mostly found on the upper
647 slopes, and grassland in the flood plains, large amounts of MP are transported from arable land to
648 grassland (Tab. 3). No tillage takes place in grassland, leading to high MP concentration in the topsoil.
649 Along the main river in particular, grassland contaminated with MP (example shown in Fig. 6f) offers a

650 high potential for MP loss during flood events. In the flood plains, the groundwater level is regularly
651 close to the surface, hence the chance of MP leaching to the groundwater increases (Chia et al., 2021;
652 Singh and Bhagwat, 2022; Viaroli et al., 2022).

653 This analysis not only sheds light on the model's impact on MP distribution in varied landscape
654 contexts but also underscores the potential environmental repercussions. The study significantly
655 advances scientific understanding and practical relevance by emphasizing long-term field experiments
656 and meso-scale model analyses. Nevertheless, gaps persist in MP research, particularly concerning
657 standardized detection methods and quantification of terrestrial MP pollution. Addressing these gaps
658 requires extensive additional research to comprehensively grasp the scope of MP pollution across diverse
659 environmental media and the entirety of the MP cycle. Substantial measurements and fundamental
660 research in this domain are imperative to enhance process comprehension and refine model applications.

661 *4.4. Soil erosion as a potential MP source for inland waters*

662 Comparing the annual MP input to arable land and the annual MP loss through soil erosion indicates
663 that only a very small proportion ($\leq 0.17\%$ since 1950) is delivered to the stream network. The loss rate
664 of TW (0.11%) was the smallest compared to sewage sludge, compost and atmospheric deposition (Tab.
665 3). This is because the TW was not applied to all fields, but only to the fields next to a road. The low
666 percentage of input lost to the streams should not lead to the fallacy that MP transport via soil erosion is
667 negligibly small (Schell et al., 2022; Weber et al., 2022). This becomes clearer when comparing the MP
668 input from soil erosion with the MP input from wastewater treatment plants (WWTP) in the study area
669 (Fig. 5). Based on the known number and size of the WWTPs in the study area and MP loads in German
670 WWTPs from literature (Mintenig et al., 2014), the MP delivery into the Glonn through WWTP outlets
671 can be estimated at an average of 25 kg MP a^{-1} (min.: 1.9 kg, max.: 49 kg) in 2020 (Fig. 5). These values
672 represent a maximum scenario since the calculations were based on the possible full capacities of the

673 WWTPs. Within the test catchment, the MP delivery into the stream network was 6.3 kg MP a⁻¹ (min.:
674 2.2 kg, max.: 21 kg) in 2020, but (S1, Fig. 5b) could reach 25.2 kg MP a⁻¹ (min.: 9 kg, max.: 84.3 kg) by
675 the end of the century (Fig. 5b).

676 Rehm et al. (2021) have shown that due to its low density, MP is preferentially eroded and is enriched
677 by up to a factor of four in delivered sediments. These potential enrichment effects were not included in
678 SPEROS-MP. In addition, other MP input sources such as plastic used in agriculture (e.g. mulch films)
679 and littering were not considered in this study. In this regard, the modeled MP delivery is therefore an
680 underestimated estimation. Overall, our results are in line with other, larger-scale model estimates for
681 the Bavarian section of the Danube catchment, showing that the MP input via soil erosion into water
682 bodies in rural areas outweighs the MP input of WWTP outlets (Witzig et al., 2021). It should therefore
683 not be claimed that soil erosion for MP transport is negligible (Schell et al., 2022) while wastewater
684 treatment plants are treated as a major MP source for inland waters (Cai et al., 2022; Eibes and Gabel,
685 2022; Murphy et al., 2016).

686 *4.5. The MP sink function of soil results in a long-term MP source*

687 Today's MP pollution of arable land represents a long-term MP source for inland waters. With the
688 model scenarios S1 and S3, this study was able to show that the MP discharge from arable soils into
689 inland waters via soil erosion will still affect many generations to come, even if MP entry into the
690 terrestrial environment could be avoided. Because of low MP loss rates ($\leq 0.17\%$) via soil erosion and
691 the stability of conventional plastic materials over centuries (Ng et al., 2018), the MP particles
692 accumulate in the soil over the years. As most of the MP stays in the plough layer (Tab. 3), it is made
693 available to surface runoff and erosion processes on a regular basis. After 80 years without MP input in
694 S3, MP delivery from the soil decreased only by 14%. The MP concentration in the topsoil of arable land
695 decreases over time due to lateral MP loss into the stream network or into neighbouring grassland and

696 forest areas (example shown in Fig. 6f). The MP concentration in the topsoil also decreases since erosion
697 and tillage incorporates MP-free subsoil and, on the other hand, MP gets below the plough layer at
698 depositional sites (outside the range of water erosion). It is important to note that tillage erosion plays an
699 important role, as it supports the burial of MP below the plough layer (example shown in Fig. 6e).

700 S3 is reminiscent of other well-known environmental problems of long-term diffuse pollution, e.g.
701 with phosphorus (Daneshgar et al., 2018; Vaccari, 2009), where a pollutant accumulates in soils but
702 slowly find its way into inland waters through soil erosion. In this respect, it is important to note that it
703 will be easier to reduce MP inputs to stream networks coming from point sources, e.g. WWTP, whereas
704 the diffuse input will continue for centuries.

705 *4.6. Targeted application of MP-laden organic fertilizer*

706 The predicted increase in plastics production means that more MP inputs into the environment can be
707 expected in the future (Borrelle et al., 2020; Horton, 2022). Because of this, it is necessary to consider
708 what measures can be taken to reduce or avoid the entry of MP into the various environmental
709 compartments. The results of S2 have shown that the application of organic fertilizer (without TW)
710 containing MP at a distance of more than 100 m from the stream network can reduce MP entry into
711 surface waters via soil erosion by up to 46% compared to S1 (Fig. 7). By contrast (unplanned) application
712 of MP-laden soil amendments in the proximity of the stream network increase MP supply (by 53% in
713 our scenario).

714 This highlights the potential impact of optimized landscape management taking into account the
715 location of any agricultural management activity. It also shows that, in addition to soil conservation in
716 the field to prevent soil erosion, general changes in catchment management affecting hydrological and
717 sedimentological connectivity have important implications for the transport of sediments and pollutants.

718 Therefore, the location of soil additives, which are usually used to close production cycles, should be
719 considered for future use. This consideration can have a significant influence on the subsequent erosion
720 transport and redistribution of, for example, MP within a whole river catchment.

721 **5. Conclusion**

722 In this study, the transport of MP eroded from arable land was modelled across a mesoscale landscape.
723 Sewage sludge, compost, atmospheric deposition and tyre wear were considered as MP sources. Tyre
724 wear not only represented the largest MP input to arable land. It also generated the largest MP delivery
725 rates to the stream network, although tyre wear is not widespread on arable land, only occurring on fields
726 near the roads. In percentage terms, only a small fraction ($< 0.2\%$) of all MP applied to arable land ended
727 up directly in the stream network via soil erosion. However, the MP mass delivered into the stream
728 network represented a serious amount of MP input. The modelled MP delivery into the stream network
729 was in the same range of potential MP inputs from wastewater treatment plants from this rural area.

730 In addition, it was shown that most of the MP applied to arable soils remains in the topsoil (0–20 cm)
731 for decades. Tillage produces a regular homogenization, and the MP stays available for surface runoff
732 and water erosion in the long term. Based on a series of scenarios modelled up to 2100 with no more MP
733 input from 2020 onwards, similar MP delivery rates (compared to 2020) could still be identified. This
734 implies that arable land represents an MP sink on the one hand and a long-term MP source for inland
735 waters on the other.

736 Using the soil profile update component included in the SPEROS-MP model, the MP concentrations
737 along the soil profile could be determined to a depth of 1 m. It was modelled that 5% of the MP applied
738 to arable land is translocated into the subsoil (> 20 cm) by tillage and water erosion. Located below the
739 plough horizon, the MP is out of reach for future lateral surface runoff erosion processes. Based on the

740 spatially distributed erosion model, it was also demonstrated that most of the eroded MP leaving arable
741 land is deposited in grassland (1% of applied MP). Especially in areas of the river valleys, these
742 accumulations could represent a concentrated MP entry into the stream network in the event of a flood.

743 The most effective protection for arable land would probably be to limit or ban the application of MP-
744 contaminated organic fertilizers. The following measures would be conceivable to protect water bodies
745 from MP inputs through soil erosion. Our model scenario showed that the targeted application of MP-
746 contaminated organic fertilizer at a distance of at least 100 m from the water body led to a significantly
747 lower MP delivery rate from this MP source. The deliberate creation of grass strips in the landscape to
748 protect against erosion would also be an option. However, it is important to consider that all calculated
749 and modelled cases were dominated by tyre wear, which is difficult to manage, especially in regions with
750 a high population and dense road network. Therefore, in order to preserve soil as a valuable resource, as
751 well as to protect the terrestrial and aquatic ecosystem from MP pollution and its effects, we should focus
752 on limiting MP emissions to the environment in general as much as possible.

753

754 **Data availability**

755 All raw data can be provided by the corresponding authors upon request.

756

757 **Author contributions**

758 Raphael Rehm: Writing - Original Draft, Data curation, Analysis, Investigation, Visualization,
759 Methodology

760 Peter Fiener: Conceptualization, Supervision, Resources, Analysis, Validation, Writing Review
761 & Editing, Funding acquisition

762

763 **Competing interests**

764 Some authors are members of the editorial board of journal SOIL. The peer-review process
765 was guided by an independent editor, and the authors have also no other competing interests
766 to declare.

767 **Acknowledgments**

768 The authors would like to acknowledge the financial support from the Federal Ministry of Education
769 and Research towards this research as part of the initiative Plastics in the Environment (funding number
770 02WPL1447A-G). In addition, we would like to thank the Bavarian State Office of Agriculture (LfL)
771 and the Bavarian State Office for the Environment (LfU) for providing and accessing Bavaria-wide data,
772 as well as providing the modelling data for the Glonn catchment area. Finally, special thanks go to the
773 members of the Soil and Water Resources Research Group in Augsburg for supporting this work.

774 **Financial support**

775 This work was supported by the Federal Ministry of Education and Research towards this
776 research as part of the initiative Plastics in the Environment (funding number 02WPL1447A-G)

777 **Review statement**

778 This paper was edited by Jan Vanderborght and reviewed by two anonymous referees.

779

780 **References**

781

- 782 Accinelli C, Abbas HK, Bruno V, Vicari A, Little NS, Ebelhar MW, et al. Minimizing abrasion losses from film-
783 coated corn seeds. *Journal of Crop Improvement* 2021; 35: 666-678.
- 784 Aves AR, Revell LE, Gaw S, Ruffell H, Schuddeboom A, Wotherspoon NE, et al. First evidence of microplastics
785 in Antarctic snow. *The Cryosphere* 2022; 16: 2127-2145.
- 786 Baensch-Baltruschat B, Kocher B, Kochleus C, Stock F, Reifferscheid G. Tyre and road wear particles-A
787 calculation of generation, transport and release to water and soil with special regard to German roads.
788 *Science of The Total Environment* 2020; 752: 141939.
- 789 BAYSIS BS. *Straßenverkehrszählungen (SVZ)*, 2015.
- 790 Bertling J, Zimmermann T, Rödiger L. *Kunststoffe in der Umwelt: Emissionen in landwirtschaftlich genutzte Böden.*
791 *Fraunhofer UMSICHT* 2021: 220.
- 792 Bläsing M, Amelung W. Plastics in soil: Analytical methods and possible sources. *Science of the Total*
793 *Environment* 2018; 612: 422-435.
- 794 Borrelle SB, Ringma J, Law KL, Monnahan CC, Lebreton L, McGivern A, et al. Predicted growth in plastic waste
795 exceeds efforts to mitigate plastic pollution. *Science* 2020; 369: 1515-1518.
- 796 Borthakur A, Leonard J, Koutnik VS, Ravi S, Mohanty SK. Inhalation risks of wind-blown dust from biosolid-
797 applied agricultural lands: Are they enriched with microplastics and PFAS? *Current Opinion in*
798 *Environmental Science & Health* 2022; 25: 100309.
- 799 Brahney J, Hallerud M, Heim E, Hahnenberger M, Sukumaran S. Plastic rain in protected areas of the United States.
800 *Science* 2020; 368: 1257-1260.
- 801 Brandes E. *Die Rolle der Landwirtschaft bei der (Mikro-) Plastik-Belastung in Böden und Oberflächengewässern.*
802 2020.
- 803 Brandes E, Henseler M, Kreins P. Identifying hot-spots for microplastic contamination in agricultural soils—a
804 spatial modelling approach for Germany. *Environmental Research Letters* 2021; 16: 104041.
- 805 Brandhuber R, Auerswald K, Lang R, Müller A, Treisch M. *ABAG interaktiv, Version 2.0.* Bayerische
806 Landesanstalt für Landwirtschaft, Freising. 2018.
- 807 Braun M, Mail M, Heyse R, Amelung W. Plastic in compost: Prevalence and potential input into agricultural and
808 horticultural soils. *Science of The Total Environment* 2021; 760: 143335.
- 809 Bullard JE, Ockelford A, O'Brien P, Neuman CM. Preferential transport of microplastics by wind. *Atmospheric*
810 *Environment* 2021; 245: 118038.
- 811 Cai Y, Wu J, Lu J, Wang J, Zhang C. Fate of microplastics in a coastal wastewater treatment plant: Microfibers
812 could partially break through the integrated membrane system. *Frontiers of Environmental Science &*
813 *Engineering* 2022; 16: 1-10.
- 814 Chia RW, Lee J-Y, Kim H, Jang J. Microplastic pollution in soil and groundwater: a review. *Environmental*
815 *Chemistry Letters* 2021; 19: 4211-4224.
- 816 Colin G, Cooney J, Carlsson D, Wiles D. Deterioration of plastic films under soil burial conditions. *Journal of*
817 *Applied Polymer Science* 1981; 26: 509-519.
- 818 Corcoran PL. Degradation of microplastics in the environment. *Handbook of Microplastics in the Environment.*
819 Springer, 2022, pp. 531-542.
- 820 Daneshgar S, Callegari A, Capodaglio AG, Vaccari D. The potential phosphorus crisis: resource conservation and
821 possible escape technologies: a review. *Resources* 2018; 7: 37.
- 822 Desmet P, Govers G. A GIS procedure for automatically calculating the USLE LS factor on topographically
823 complex landscape units. *Journal of soil and water conservation* 1996; 51: 427-433.
- 824 Dlugoß V, Fiener P, Van Oost K, Schneider K. Model based analysis of lateral and vertical soil carbon fluxes
825 induced by soil redistribution processes in a small agricultural catchment. *Earth Surface Processes and*
826 *Landforms* 2012; 37: 193-208.
- 827 DWD DW. *Klimadaten direkt zum Download. 3. Rasterfelder für Deutschland.* 2020.
- 828 Edo C, González-Pleiter M, Leganés F, Fernández-Piñas F, Rosal R. Fate of microplastics in wastewater treatment
829 plants and their environmental dispersion with effluent and sludge. *Environmental Pollution* 2020; 259:
830 113837.

831 Eibes PM, Gabel F. Floating microplastic debris in a rural river in Germany: Distribution, types and potential
832 sources and sinks. *Science of The Total Environment* 2022; 816: 151641.

833 Feuilletoy P, César G, Benguigui L, Grohens Y, Pillin I, Bewa H, et al. Degradation of polyethylene designed for
834 agricultural purposes. *Journal of Polymers and the Environment* 2005; 13: 349-355.

835 Fiener P, Dlugoš V, Van Oost K. Erosion-induced carbon redistribution, burial and mineralisation - Is the episodic
836 nature of erosion processes important? *Catena* 2015; 133: 282-292.

837 Fiener P, Dostál T, Krása J, Schmaltz E, Strauss P, Wilken F. Operational USLE-Based Modelling of Soil Erosion
838 in Czech Republic, Austria, and Bavaria—Differences in Model Adaptation, Parametrization, and Data
839 Availability. *Applied Sciences* 2020; 10: 3647.

840 Fiener P, Govers G, Van Oost K. Evaluation of a dynamic multi-class sediment transport model in a catchment
841 under soil-conservation agriculture. *Earth Surface Processes and Landforms* 2008; 33: 1639-1660.

842 Fiener P, Wilken F, Aldana-Jague E, Deumlich D, Gómez J, Guzmán G, et al. Uncertainties in assessing tillage
843 erosion—how appropriate are our measuring techniques? *Geomorphology* 2018; 304: 214-225.

844 Frias JP, Nash R. Microplastics: Finding a consensus on the definition. *Marine pollution bulletin* 2019; 138: 145-
845 147.

846 Gehrke I, Dresen B, Blömer J, Sommer H, Lindow F, Röckle R. TyreWearMapping. Digitales Planungs-und
847 Entscheidungsinstrument zur Verteilung, Ausbreitung und Quantifizierung von Reifenabrieb in
848 Deutschland. Schlussbericht. 2021.

849 Govers G, Vandaele K, Desmet P, Poesen J, Bunte K. The role of tillage in soil redistribution on hillslopes.
850 *European Journal of Soil Science* 1994; 45: 469-478.

851 Guo J-J, Huang X-P, Xiang L, Wang Y-Z, Li Y-W, Li H, et al. Source, migration and toxicology of microplastics
852 in soil. *Environment International* 2020; 137: 105263.

853 Habib RZ, Thiemann T, Al Kendi R. Microplastics and wastewater treatment plants—a review. *Journal of Water
854 Resource and Protection* 2020; 12: 1.

855 Heinze WM, Mitrano DM, Cornelis G. Bioturbation-driven transport of microplastic fibres in soil. *Copernicus
856 Meetings*, 2022.

857 Hillenbrand T, Toussaint D, Boehm E, Fuchs S, Scherer U, Rudolphi A, et al. Discharges of copper, zinc and lead
858 to water and soil. Analysis of the emission pathways and possible emission reduction measures; Eintraege
859 von Kuper, Zink und Blei in Gewaesser und Boeden. Analyse der Emissionspfade und moeglicher
860 Emissionsminderungsmassnahmen. 2005.

861 Horton AA. Plastic pollution: When do we know enough? *Journal of Hazardous Materials* 2022; 422: 126885.

862 Huerta Lwanga E, Thapa B, Yang X, Gertsen H, Salanki T, Geissen V, et al. Decay of low-density polyethylene
863 by bacteria extracted from earthworm's guts: A potential for soil restoration. *Sci Total Environ* 2017; 624:
864 753-757.

865 Hurley RR, Nizzetto L. Fate and occurrence of micro(nano)plastics in soils: Knowledge gaps and possible risks.
866 *Current Opinion in Environmental Science & Health* 2018; 1: 6-11.

867 Keller B, Centeri C, Szabó JA, Szalai Z, Jakab G. Comparison of the applicability of different soil erosion models
868 to predict soil erodibility factor and event soil losses on loess slopes in Hungary. *Water* 2021; 13: 3517.

869 Kim Y-N, Yoon J-H, Kim K-HJ. Microplastic contamination in soil environment—a review. *Soil Science Annual
870 2021*; 71: 300-308.

871 Klein M, Fischer EK. Microplastic abundance in atmospheric deposition within the Metropolitan area of Hamburg,
872 Germany. *Science of the Total Environment* 2019; 685: 96-103.

873 Knight LJ, Parker-Jurd FN, Al-Sid-Cheikh M, Thompson RC. Tyre wear particles: an abundant yet widely
874 unreported microplastic? *Environmental Science and Pollution Research* 2020a; 1-10.

875 Knight LJ, Parker-Jurd FN, Al-Sid-Cheikh M, Thompson RC. Tyre wear particles: an abundant yet widely
876 unreported microplastic? *Environmental Science and Pollution Research* 2020b; 27: 18345-18354.

877 Kocher B, Brose S, Feix J, Görg C, Peters A, Schenker K. Stoffeinträge in den Straßenseitenraum-Reifenabrieb.
878 BERICHTE DER BUNDESANSTALT FUER STRASSENWESEN. UNTERREIHE
879 VERKEHRSTECHNIK 2010.

880 Krasa J, Dostal T, Van Rompaey A, Vaska J, Vrana K. Reservoirs' siltation measurements and sediment transport
881 assessment in the Czech Republic, the Vrchlice catchment study. *Catena* 2005; 64: 348-362.

882 LfL BLfL. Erosionsatlas Bayern. 2023.

883 LfStaD BLfSuD. Statistisches Jahrbuch für Bayern. 2022.

884 LfU BLfU. Abfallwirtschaft–Hausmüll in Bayern–Bilanzen 2002. Bayerisches Landesamt für Umweltschutz,
885 Augsburg 1990-2020.

886 Li H, Lu X, Wang S, Zheng B, Xu Y. Vertical migration of microplastics along soil profile under different crop
887 root systems. *Environmental Pollution* 2021; 278: 116833.

888 Li S, Ding F, Flury M, Wang Z, Xu L, Li S, et al. Macro-and microplastic accumulation in soil after 32 years of
889 plastic film mulching. *Environmental Pollution* 2022; 300: 118945.

890 Lian J, Liu W, Meng L, Wu J, Zeb A, Cheng L, et al. Effects of microplastics derived from polymer-coated fertilizer
891 on maize growth, rhizosphere, and soil properties. *Journal of Cleaner Production* 2021; 318: 128571.

892 Liu EK, He WQ, Yan CR. ‘White revolution’ to ‘white pollution’—agricultural plastic film mulch in China.
893 *Environmental Research Letters* 2014; 9.

894 Lwanga EH, Beriot N, Corradini F, Silva V, Yang X, Baartman J, et al. Review of microplastic sources, transport
895 pathways and correlations with other soil stressors: a journey from agricultural sites into the environment.
896 *Chemical and Biological Technologies in Agriculture* 2022; 9: 1-20.

897 Meinen BU, Robinson DT. Agricultural erosion modelling: Evaluating USLE and WEPP field-scale erosion
898 estimates using UAV time-series data. *Environmental Modelling & Software* 2021; 137: 104962.

899 Mennekes D, Nowack B. Tire wear particle emissions: Measurement data where are you? *Science of The Total*
900 *Environment* 2022; 830: 154655.

901 Mintenig S, Int-Veen I, Löder M, Gerdt G. Mikroplastik in ausgewählten Kläranlagen des Oldenburgisch-
902 Ostfriesischen Wasserverbandes (OOWV) in Niedersachsen. 2014.

903 Motto HL, Daines RH, Chilko DM, Motto CK. Lead in soils and plants: its relation to traffic volume and proximity
904 to highways. *Environmental Science & Technology* 1970; 4: 231-237.

905 Müller A, Kocher B, Altmann K, Braun U. Determination of tire wear markers in soil samples and their distribution
906 in a roadside soil. *Chemosphere* 2022; 294: 133653.

907 Murphy F, Ewins C, Carbonnier F, Quinn B. Wastewater Treatment Works (WwTW) as a Source of Microplastics
908 in the Aquatic Environment. *Environ Sci Technol* 2016; 50: 5800-8.

909 Nadeu E, Gobin A, Fiener P, Van Wesemael B, Van Oost K. Modelling the impact of agricultural management on
910 soil carbon stocks at the regional scale: the role of lateral fluxes. *Global Change Biology* 2015: DOI:
911 10.1111/gcb.12889.

912 Nasser S, Azizi N. Occurrence and Fate of Microplastics in Freshwater Resources. *Microplastic Pollution*.
913 Springer, 2022, pp. 187-200.

914 Ng E-L, Lwanga EH, Eldridge SM, Johnston P, Hu H-W, Geissen V, et al. An overview of microplastic and
915 nanoplastic pollution in agroecosystems. *Science of the total environment* 2020; 627: 1377-1388.

916 Ng EL, Lwanga EH, Eldridge SM, Johnston P, Hu HW, Geissen V, et al. An overview of microplastic and
917 nanoplastic pollution in agroecosystems. *Science of the Total Environment* 2018; 627: 1377-1388.

918 Nunes JP, Wainwright J, Biëlders CL, Darboux F, Fiener P, Finger D, et al. Better models are more effectively
919 connected models. *Earth Surface Processes and Landforms* 2018; 43.

920 Pérez-Reverón R, González-Sálamo J, Hernández-Sánchez C, González-Pleiter M, Hernández-Borges J, Díaz-Peña
921 FJ. Recycled wastewater as a potential source of microplastics in irrigated soils from an arid-insular
922 territory (Fuerteventura, Spain). *Science of The Total Environment* 2022; 817: 152830.

923 Rehm R, Zeyer T, Schmidt A, Fiener P. Soil erosion as transport pathway of microplastic from agriculture soils to
924 aquatic ecosystems. *Science of The Total Environment* 2021; 795: 148774.

925 Rillig MC, Ziersch L, Hempel S. Microplastic transport in soil by earthworms. *Sci Rep* 2017; 7: 1362.

926 Sajjad M, Huang Q, Khan S, Khan MA, Yin L, Wang J, et al. Microplastics in the soil environment: A critical
927 review. *Environmental Technology & Innovation* 2022: 102408.

928 Schell T, Hurley R, Buenaventura NT, Mauri PV, Nizzetto L, Rico A, et al. Fate of microplastics in agricultural
929 soils amended with sewage sludge: Is surface water runoff a relevant environmental pathway?
930 *Environmental Pollution* 2022; 293: 118520.

931 Scheurer M, Bigalke M. Microplastics in Swiss Floodplain Soils. *Environmental science & technology* 2018.

932 Schleyen P. Abwasserbehandlung (nach 1945). *Historisches Lexikon Bayerns* 2017.

933 Schmidt J, v.Werner M, Michael A. Application of the EROSION 3D model to the CATSOP watershed, The
934 Netherlands. *Catena* 1999; 37: 449-456.

935 Schwertmann U, Vogl W, Kainz M. *Bodenerosion durch Wasser*. Ulmer Verlag, 64 p 1987.

936 Singh S, Bhagwat A. Microplastics: A potential threat to groundwater resources. *Groundwater for Sustainable*

937 *Development* 2022; 100852.

938 Sommer F, Dietze V, Baum A, Sauer J, Gilge S, Maschowski C, et al. Tire abrasion as a major source of

939 microplastics in the environment. *Aerosol and Air Quality Research* 2018; 18: 2014-2028.

940 StMB. *Verkehrsentwicklung*. 2023.

941 Tang KHD, Hadibarata T. Microplastics removal through water treatment plants: Its feasibility, efficiency, future

942 prospects and enhancement by proper waste management. *Environmental Challenges* 2021; 5: 100264.

943 Tian L, Jinjin C, Ji R, Ma Y, Yu X. Microplastics in agricultural soils: sources, effects, and their fate. *Current*

944 *Opinion in Environmental Science & Health* 2022; 25: 100311.

945 Unice KM, Weeber MP, Abramson MM, Reid RCD, van Gils JAG, Markus AA, et al. Characterizing export of

946 land-based microplastics to the estuary - Part I: Application of integrated geospatial microplastic transport

947 models to assess tire and road wear particles in the Seine watershed. *Science of the Total Environment*

948 2019; 646: 1639-1649.

949 Vaccari DA. Phosphorus: a looming crisis. *Scientific American* 2009; 300: 54-59.

950 Van Oost K, Govers G, De Alba S, Quine T. Tillage erosion: a review of controlling factors and implications for

951 soil quality. *Progress in Physical Geography* 2006; 30: 443-466.

952 Van Oost K, Govers G, Desmet P. Evaluating the effects of changes in landscape structure on soil erosion by water

953 and tillage. *Landscape ecology* 2000; 15: 577-589.

954 Van Oost K, Govers G, Quine TA, Heckrath G, Olesen JE, De Gryze S, et al. Landscape-scale modeling of carbon

955 cycling under the impact of soil redistribution: The role of tillage erosion. *Global Biogeochemical Cycles*

956 2005a; 19.

957 Van Oost K, Govers G, Van Muysen W. A process-based conversion model for caesium-137 derived erosion rates

958 on agricultural land: An integrated spatial approach. *Earth Surface Processes and Landforms: The Journal*

959 *of the British Geomorphological Research Group* 2003; 28: 187-207.

960 Van Oost K, Quine T, Govers G, Heckrath G. Modeling soil erosion induced carbon fluxes between soil and

961 atmosphere on agricultural land using SPEROS-C. In: Roose EJ, Lal R, Feller C, Barthes B, Stewart BA,

962 editors. *Advances in soil science. Soil erosion and carbon dynamics*. CRC Press, Boca Raton, 2005b, pp.

963 37-51.

964 Van Rompaey AJ, Verstraeten G, Van Oost K, Govers G, Poesen J. Modelling mean annual sediment yield using

965 a distributed approach. *Earth Surface Processes and Landforms* 2001; 26: 1221-1236.

966 Verstraeten G, Prosser IP. Modelling the impact of land-use change and farm dam construction on hillslope

967 sediment delivery to rivers at the regional scale. *Geomorphology* 2008; 98: 199-212.

968 Viaroli S, Lancia M, Re V. Microplastics contamination of groundwater: Current evidence and future perspectives.

969 A review. *Science of The Total Environment* 2022: 153851.

970 Wagner S, Hüffer T, Klöckner P, Wehrhahn M, Hofmann T, Reemtsma T. Tire wear particles in the aquatic

971 environment-a review on generation, analysis, occurrence, fate and effects. *Water research* 2018; 139: 83-

972 100.

973 Waldschläger K, Schüttrumpf H. Infiltration Behavior of Microplastic Particles with Different Densities, Sizes,

974 and Shapes—From Glass Spheres to Natural Sediments. *Environmental Science & Technology* 2020; 54:

975 9366-9373.

976 Weber CJ, Santowski A, Chiffard P. Investigating the dispersal of macro-and microplastics on agricultural fields

977 30 years after sewage sludge application. *Scientific reports* 2022; 12: 1-13.

978 Weithmann N, Möller JN, Löder MG, Piehl S, Laforsch C, Freitag R. Organic fertilizer as a vehicle for the entry

979 of microplastic into the environment. *Science Advances* 2018; 4: eaap8060.

980 Werkenthin M, Kluge B, Wessolek G. Metals in European roadside soils and soil solution—A review.

981 *Environmental Pollution* 2014; 189: 98-110.

982 Wheeler G, Rolfe G. The relationship between daily traffic volume and the distribution of lead in roadside soil and

983 vegetation. *Environmental Pollution* (1970) 1979; 18: 265-274.

984 Wik A, Dave G. Occurrence and effects of tire wear particles in the environment—A critical review and an initial

985 risk assessment. *Environmental pollution* 2009; 157: 1-11.

986 Witzig C, Wörle K, Földi C, Rehm R, Reuwer A-K, Ellerbrake K, et al. Mikroplastik in Binnengewässern.
987 Untersuchung und Modellierung des Eintrags und Verbleibs im Donaugebiet als Grundlage für
988 Maßnahmenplanung. MICBIN Abschlussbericht. 2021.

989 WRB IWG. World reference base for soil resources 2014, update 2015. International soil classification system for
990 naming soils and creating legends for soil maps. World Soil Resources Reports No. 106. FAO 2015.

991 Wright S, Ulke J, Font A, Chan K, Kelly F. Atmospheric microplastic deposition in an urban environment and an
992 evaluation of transport. *Environment International* 2019; 105411.

993 Zhang L, Xie Y, Liu J, Zhong S, Qian Y, Gao P. An overlooked entry pathway of microplastics into agricultural
994 soils from application of sludge-based fertilizers. *Environmental science & technology* 2020; 54: 4248-
995 4255.

996 Zhang Y, Gao T, Kang S, Shi H, Mai L, Allen D, et al. Current status and future perspectives of microplastic
997 pollution in typical cryospheric regions. *Earth-Science Reviews* 2022; 226: 103924.

998 Zhao S, Zhang Z, Chen L, Cui Q, Cui Y, Song D, et al. Review on migration, transformation and ecological impacts
999 of microplastics in soil. *Applied Soil Ecology* 2022; 176: 104486.

1000 Zhou Y, Wang J, Zou M, Jia Z, Zhou S. Microplastics in soils: A review of methods, occurrence, fate, transport,
1001 ecological and environmental risks. *Science of The Total Environment* 2020: 141368.

1002 Zubris KA, Richards BK. Synthetic fibers as an indicator of land application of sludge. *Environ Pollut* 2005; 138:
1003 201-11.

1004